
# Optimizing biofuel production: Direct integration and co-hydroprocessing of hydrolysis lignin into oil refineries over an unsupported NiMoP catalyst

Energy Conversion and Management 327 (2025) 119606

Contents lists available at ScienceDirect

Energy Conversion and Management

journal homepage: www.elsevier.com/locate/enconman

# Optimizing biofuel production: Direct integration and co-hydroprocessing of hydrolysis lignin into oil refineries over an unsupported NiMoP catalyst

Abdenour Achour *, Anna Anttila, Derek Creaser, Louise Olsson *

*Competence Centre for Catalysis, Chemical Engineering, Chalmers University of Technology SE 412 96 Gothenburg, Sweden*

ARTICLE INFO

*Keywords:*
Co-hydroprocessing
Hydrolysis lignin
Drop-in fuel
unsupported NiMoP catalyst

ABSTRACT

Our study investigates the production of drop-in fuels by co-hydroprocessing solid hydrolysis lignin in a batch reactor operated in cycling mode. To simulate the blending potential with lignin oil, we utilized petroleum-derived intermediates like hexadecane and VGO. We demonstrate the significant production of blended lignin-oil through direct co-hydroprocessing of hydrolysis lignin and its hydroprocessed oil using a spent catalyst. The reactivity of hydrolysis lignin is influenced by its interaction with organic mediators in the lignin-oil blends. For hydrotreated lignin in hexadecane, we observed an 83.4 wt% yield of lignin monomers, predominantly isomeric alkane-derived, including cycloalkanes. Co-hydroprocessing with fresh lignin increased lignin-oil blend yield and reduced char formation. Additionally, the NiMoP loading significantly boosted naphtha and light gas oil yields. Co-hydroprocessing with VGO exhibited a slightly higher yield of 85.6 wt%, accompanied by a significantly lower char yield of 1.6 wt% compared to the uncatalyzed reaction, which yielded 33.7 wt% char. The enhanced reactivity and affinity with VGO resulted in improved selectivity towards naphthenes and aromatics. Overall, higher catalyst loadings promoted dealkylation and deoxygenation reactions while suppressing char formation, remarkably evident with VGO in multicycling. Interestingly, multicycling led to a higher bio-oil yield and lower char formation. Furthermore, our study suggests that co-hydroprocessing with intermittent feeding of hydrolysis lignin in a sequential operation mode can achieve deep deoxygenation, higher energy yield, and mass lignin-oil yields while maximizing the distillate range of jet and marine fuel fractions, as qualitatively evident using funnel plots.

## 1. Introduction

The depletion of fossil fuel resources drives the demand for alternative energy resources [1]. Biomass, affordable and abundant, can be converted into a wide range of products, including biofuels, electricity, heat, and chemicals through various conversion pathways [2]. However, scaling up production faces economic challenges, particularly given the significant demand in the transport sector [2–4]. To accelerate this transition, co-processing biomass-derived materials in existing oil refineries is a paramount step to ensure the consistent quality of final fuels [5]. In order to establish a massive-scale biofuel system in the short term, the co-processing of biomass derived resources in oil refineries could be a realistic and economic scenario [1,2,6]. Several process technologies have been developed to upgrade vacuum residue and heavy oils into light fractions [7], encompassing carbon rejection and hydrogen addition processes, including visbreaking, steam cracking, fluid catalytic cracking (FCC), fixed-bed catalytic hydroconversion, and slurry-bed catalytic hydroconversion [2,5,7,8]. Among these technologies, slurry-phase hydroconversion stands out as a promising process, facilitating better contact between the catalyst and feedstock, resulting in higher conversion rates [9]. Co-processing lignin-biomass and liquid-biocrudes in these systems with oil refineries can occur at various locations, depending on the nature of the biocrude and the target product. Numerous developments regarding co-processing are reported in research publications, patents, and international consortiums projects [2,5–8,10].

Much effort has been focused on co-processing bio-oils generated from fast pyrolysis and hydrothermal liquefaction (HTL) with petroleum-derived feedstocks in FCC, hydrotreater, or hydrocracker processes [11,12]. The aim is to utilize these bio-oils for the production of sustainable marine and aviation fuels in the future. The FCC insertion point offers economic attractiveness, yet unacceptable increases in temperature due to excess coke production resulting from the poor thermal stability of bio-oils, leading to damage of the FCC catalyst, and

* Corresponding authors.
*E-mail addresses:* abdenour@chalmers.se (A. Achour), louise.olsson@chalmers.se (L. Olsson).

https://doi.org/10.1016/j.enconman.2025.119606
Received 28 October 2024; Received in revised form 11 January 2025; Accepted 31 January 2025
Available online 5 February 2025

therefore posing a challenge to maintain an appropriate heat balance [13–16]. This necessitates a stabilization step before injection into the FCC reactor. Several researchers have conducted catalytic hydrotreating of the bio-oil, reducing its oxygen content close to 5 %, before co-processing it with light cycle oil (LCO) and vacuum gas oil (VGO) [17,18]. This upgrading step primarily involves converting cellulose-derived sugars in the bio-oil into alcohols, which are less prone to form coke. de Miguel Mercader *et al.* co-processed 20 wt% hydrotreated bio-oil in fossil fuel and compared with the result obtained from pure hydrotreated bio-oil [19]. It was found that this was still possible with only a 7.8 % increase in coke formation. It was found that internal hydrogen transfer, causing a reduction in the coke precursor concentration during the co-processing of the renewable and fossil feed, could be potentially operative mechanisms to explain these results. However, they concluded that, to date, it is not possible to determine which mechanism causes the changes in the yield profile [19]. Catalytic pyrolysis has also been used to stabilize the bio-oil before co-processing [18,20–24]. Similar results as for hydrotreated bio-oil have been reported, except for a higher coke yield in the catalytic pyrolysis due to the presence of more unsaturated compounds [25]. Other challenges arise from difficulties in dispersing, and atomizing the bio-oil, which may transform into coke on the catalyst and block its active sites [17,18,20,22,23]. Recently, Melin et al. found that limiting the co-processing biocrude to about 10 % in VGO had little impact on the naphtha yields without a significant change in the coke yield [26].

Research on co-hydrotreating and hydrocracking of bio-oils remains limited. de Miguel Mercader et *al.* studied co-hydrotreating bio-oils with petroleum gas oils [19]. They found that the reduction in desulfurization activity was due to competition with the catalytic hydrodeoxygenation (HDO) reactions, not irreversible Ru/C catalyst deactivation. The resulting molecular weight distribution of a co-processed HDO/fossil oil blend resembled that of hydrotreated fossil oil, regardless of the origin of the HDO oil [19]. Pinheiro et *al.* observed inhibition of gas oils co-hydrotreatment reactions in the presence of bio-oil fractions using a $CoMo/Al_2O_3$ catalyst [27]. CO and $CO_2$ from decarboxylation and decarbonylation of esters and carboxylic acids inhibited catalytic reactions, suggesting the need for a $CO/CO_2$ insensitive catalyst or one favoring dehydration for effective de-oxygenation hydrotreatment. Co-hydrotreatment with a renewable oil like canola was suggested. Han et *al.* experimented with co-hydrotreating the lignin-rich oil phase over $CoMo/Al_2O_3$ and observed increased coke yield with a higher lignin-rich oil content [28]. Introducing 1-butanol as a hydrogen donor before blending, reduced coke formation, although it remained higher compared to hydrotreating canola oil alone. Catalytic co-processing of HTL biocrude with rapeseed oil over $NiMo/Al_2O_3$ showed no oxygen content and a micro-carbon residue, resembling the boiling range of biodiesel [28]. Optimal refinery advantages unfold when introducing bio-oil post-mild upgrading into select processing units [28]. Both cracking and the capability to remove oxygen from the biocrude is required from these processing units, and therefore, co-processing could potentially take place in the FFC, hydrotreater, or hydrocracker. In their study, Alvares-Majmutov *et al.* explored the co-hydrocracking of deoxygenated bio-oil alongside VGO over a $MoS_2$ unsupported catalyst that yielded naphtha and diesel in quantities similar to those from VGO [29]. The catalyst showed no signs of deactivation throughout an extensive 2154-hour testing period. These findings underscore the viability of co-hydrocracking bio-oils, particularly those that have undergone prior hydrotreatment. As noted in studies by Grilc et al. [30], unsupported $MoS_2$ catalyst exhibited higher activity compared to their $MoS_2$(IF)/C counterparts due to their influence of different morphology, including surface area and better dispersion of active sites. Among these, $MoS_2$ demonstrated the highest activity and selectivity towards hydrodeoxygenation. Furthermore, when compared to a commercially available $NiMo/\gamma\text{-}Al_2O_3$ catalyst with similar $MoS_2$ loading, the hydroxyl group removal rate was comparable; however, unsupported $MoS_2$ showed much greater selectivity for deoxygenation through hydrogenolysis. This highlights the advantage of unsupported $MoS_2$ catalysts in achieving selective and efficient deoxygenation.

Research on the co-hydrotreating liquefaction of solid lignin with petroleum feed remains relatively limited. Recently, Cheah et *al.* introduced a new strategy to suppress char formation by slurry co-hydroprocessing of Kraft lignin and pyrolysis oil in a paraffinic solvent [31]. The observed char suppression was attributed to the synergistic effects of functional groups found in the lignin-derived products. Deneyer et *al.* demonstrated the possibility to produce compatible biogasoline by integrating real lignocellulosic feedstock in two catalytic steps in an existing petrorefinery facility that targeted 10 % bio-based carbon [32]. Another important driver for studying unsupported catalysts is their potential application in upgrading heavy oils [33]. In hydrotreating heavy oils containing residual matter, supported catalysts used in conventional fixed-bed processes are prone to deactivation due to coke deposition on their surfaces [34]. Unsupported catalysts, in contrast, exhibit minimal deactivation issues because they can function as once-through catalysts. Furthermore, unsupported catalysts demonstrate higher catalytic activity, attributed to their high active material loading and large exposed surface area. These advantages position unsupported catalysts as promising candidates for use in slurry-phase processes in heavy oil refineries [33,35]. Slurry-phase systems are more adaptable to varying reaction conditions and provide superior heat transfer and catalyst recovery compared to fixed-bed systems. Additionally, the use of unsupported catalysts in slurry systems facilitates easier catalyst regeneration, which is critical for maintaining long-term operational efficiency in industrial settings [33,35]. Furthermore, the inclusion of phosphorus (P) as a promoter in NiMoP catalysts provides a greener alternative to traditional catalysts. Unlike conventional NiMo catalysts that require sulfiding for activation, NiMoP can be used without the need for sulfiding, reducing the environmental impact of catalyst preparation. The phosphorus acts as a promoter that stabilizes the active sites and enhances hydrogenation activity, as demonstrated by Wang et al. [36], who found that P-modified $Ni_2P$ catalysts exhibited excellent performance without requiring sulfiding, making them more sustainable and easier to handle. Incorporating lignin-oil produced via catalytic hydrotreating in petroleum fuels as finished fuels may represent the lowest risk for refineries if complete oxygen and char suppression is ensured. Several issues may affect the economic and operational viability of co-processing, including the stability, quality, and availability of large quantities of biogenic feedstocks. Improving the conversion of residual lignin, such as hydrolysis lignin has recently received attention due to its potential to provide high yields of lignin-oil due to its higher reactivity and lower sulfur and ash contents compared to Kraft lignin [37]. Studies have often reported that relatively high aromatic yields can be achieved.

The effect of depolymerization of hydrolysis lignin under various reaction conditions has been studied through a semi-continuous process over a sulfided $NiMo/\gamma\text{-}Al_2O_3$ catalyst [38]. The major product of hydrolysis lignin hydrogenation consisted mainly of aromatics, naphthenes, and phenols under 380 °C, and 70 bar $H_2$. In another catalytic conversion study, performed over a 5 wt% Ni/AC catalyst, an aromatic monomer yield of 12.1 wt% was obtained from hydrolysis lignin at 240 °C for 4 h with 30 bar $H_2$ in methanol [39]. Tymchyshyn *et al.* studied the hydrogenation of hydrolysis lignin used a MoRu/AC catalyst and found that the presence of acetone solvent lowered the molecular weight of the bio-oils (380 g/mol average) with high yields of around 85 wt% at 340 °C [40]. Recently, Sang *et al.* found that hydrolysis lignin when completely converted to lignin-oil, gave the highest monomer yield of 28.9 % over an unsupported Ni catalyst in supercritical ethanol at 280 °C for 6 h with 20 bar $H_2$ [41]. More recently, we evaluated the catalytic depolymerization of hydrolysis and Kraft lignin over a non-supported NiMoS catalyst alongside hexadecane [37]. The results found that the yield of monomeric compounds was nearly 76 and 47 wt % for hydrolysis and Kraft lignins, respectively. We suggested that the high performance of hydrolysis lignin is related to its chemical structure

and reactivity. This study showed that a deep removal of the oxygen-containing functional groups could be obtained, while steering the H/C ratio and improving the overall carbon yield [37].

Hydrolysis lignin, a byproduct from enzymatic hydrolysis during bioethanol production, has recently emerged as a promising feedstock for advanced biofuels. Enzymatic hydrolysis, which converts lignocellulosic biomass into fermentable sugars for bioethanol production, also generates a lignin fraction that is often underutilized. Industrial lignin hydrolysis processes, such as those employed by companies like SEKAB's Biorefinery Process, Clariant's Sunliquid Process, and Beta Renewables' PROESA Technology. These processes aim to maximize the separation of lignin from cellulose and hemicellulose, ensuring that lignin is recovered in a high-quality form suitable for downstream upgrading. Moreover, the integration of hydrolysis lignin into the biorefinery model, where lignin is upgraded to valuable biofuels and chemicals, has gained attention due to its potential to reduce refinery waste while producing high-value products.

This present work addresses a significant research gap by investigating the production of drop-in fuels with a direct upstream integration of hydrolysis lignin, a co-product of the bio-ethanol production process, into co-hydroprocessing in existing petrorefineries. Our research marks the first investigation, to the best of our knowledge, of hydrolysis lignin's potential in co-hydroprocessing alongside petroleum intermediates, knowing its ability to yield high-quality and ultra-low-sulfur lignin-oil. Utilizing an unsupported nickel-molybdenum-phosphorus (NiMoP) catalyst, we investigate the hydroprocessing effect of hydrolysis lignin residue in oil refineries, with a primary focus on product distribution and distillate fractions. Additionally, we aim to elucidate the influence of operational conditions and lignin capacity on the upgraded lignin-oil selectivity. Furthermore, we investigate a novel approach to intermittently co-hydroprocess fresh hydrolysis lignin residue with spent catalyst and lignin-oil blends. In this work, we also introduce a funnel plot that compares the characteristics of the produced lignin-oil blends, encompassing the product quality, deoxygenation degree, distillate range fractions (177 – 343 °C) and the mass and energy yields.

## 2. Experimental

### 2.1. Feedstocks and chemicals

The feedstocks and chemicals used in this study were carefully selected and prepared to ensure consistency and reliability in the experiments. Hydrolysis lignin, kindly provided by Sekab (Sweden), was pre-dried at 80 °C in an oven before being ground and sieved to achieve a particle size of 180 μm. Vacuum gas oil (VGO) was gently warmed in a water bath set to 50 °C to facilitate its transfer into the reactor. The properties of hydrolysis lignin, hexadecane, and VGO are presented in Table 1. For catalyst synthesis, we used ammonium molybdate tetrahydrate (81–83 % MoO3 basis), nickel (II) nitrate hexahydrate (99 %), ammonium dihydrogen phosphate (98 %), mesoporous SBA-16 (pore size 5 nm), ethanol (Reagent Plus®, 99 %), and sodium hydroxide (NaOH, 97 %), all supplied by Sigma-Aldrich. The chemicals employed in hydroconversion reactions and product recovery included hexadecane (Reagent Plus®, 99 %), acetone (MERCK, EMSURE®, ≥99.8 %), and dimethyl sulfoxide (DMSO, Reagent Plus®, 99 %). All chemicals were of analytical grade and used without additional purification.

### 2.2. Preparation of the catalysts

The unsupported NiMoP catalyst was synthesized via a nanocasting technique employing mesostructured silica as a hard template, following a procedure outlined in our recent publication [37]. SBA-16, comprising solely silica, served as the templates. Hard templating, a pivotal strategy for crafting crystalline mesoporous materials, leverages the distinctive structure of the hard template to inhibit precursor crystallization or aggregation. A mixture consisting of metal precursors– 0.5 g of ammonium molybdate (VI) tetrahydrate, 0.3 g of ammonium dihydrogen phosphate, and 3.5 g of nickel (II) nitrate hexahydrate–in a molar ratio of 1:1:4 was dissolved in 100 mL of ethanol. Mesoporous SBA-16 was dispersed into the aqueous precursor mixture while stirring at room temperature for 2 h. Subsequently, the solvent was gradually evaporated using a water bath set at 65 °C and a slow stirring rate. The resulting paste catalyst was then subjected to heating at 200 °C for 6 h. The solid obtained was dissolved once again in absolute ethanol and infiltrated into the channel of 1.5 g of the mesoporous SBA-16. Following re-impregnation and removal of ethanol, the solid obtained underwent calcination at 450 °C for 6 h at a heating rate of 6 °C/min. The mesostructured SBA-16 template was then removed by treating the solid with a 0.5 M NaOH solution multiple times. The resulting green solid was subsequently washed with distilled water, dried at 80 °C, and designated as NiMoP.

**Table 1**
Properties of hydrolysis lignin, hexadecane and VGO.

| Property | hydrolysis lignin [32] | HT-hexadecane | VGO* |
|---|---|---|---|
| density at 15.6°C, g/cm$^3$ | – | 0.7733 | 0.9752 |
| carbon, wt.% | 55.9 | 80.5 | 86.6 |
| hydrogen, wt.% | 5.7 | 19.9 | 12.9 |
| oxygen, wt.% | 38.1 | – | 0.2 |
| nitrogen, wt.% | 0.3 | – | 0.1 |
| sulfur, wt.% | 0.08 | – | – |
| ash, wt.% | 0.5 | – | – |
| moisture, wt.% | 1.5 | – | – |
| *SimDis TGA** | | | |
| naphtha range (wt.%, IBP-177°C) | – | 8.7 | 0.35 |
| distillate range (wt.%, 177–343 °C) | – | 91.3 | 25.0 |
| heavy oil range (wt.%, 343–524 °C) | – | 0 | 74.0 |
| residue (wt.%, > 524 °C) | – | 0 | 0.65 |

* SimDist–TGA carried out from 30 °C to 750 °C at a rate of 50 °C/min under $N_2$ flow of 50 mL/min.
[32] properties published from previous work.

### 2.3. Catalyst characterization

The physicochemical properties of the synthesized catalysts were evaluated using X-ray diffraction (XRD), $N_2$ adsorption, and chemical analyses. Detailed descriptions of these techniques can be found in our previously published work [37]. The porosity and surface area of the catalyst were determined via $N_2$-physisorption using a TriStar 3000 analyzer. Prior to measurement, the catalysts were degassed at 300 °C for 12 h under a flow of nitrogen gas. Powder X-ray diffraction (XRD) patterns were acquired using a D8 Advance Bruker with Cu Kα radiation (λ = 1,542 Å) over a 2θ range of 20-80° at a rate 1°/min. Thermogravimetry analysis (TGA) was performed using a TGA/DSC 3 + Star analyzer (Mettler Toledo, Switzerland). High-resolution transmission electron microscope (HRTEM) imaging was carried out utilizing a FEI Titan 80–300 microscope with a field emission gun, a probe Cs corrector, and a Gatan image filter Tridium, operating at 300 kV. Ammonia temperature-programmed desorption ($NH_3$-TPD) analysis was conducted using a Differential Scanning Calorimeter (DSC, Setaram Sensys). Gas flow was regulated by mass flow controllers (MFC, Bronkhorst), with outlet gases quantified using a mass spectrometer (MS, Hiden Analytical HPR 20). X-ray photoelectron spectra (XPS) analysis was carried out using PerkinElmer PHI 5000 Versa Probe III. This spectrometer uses a monochromatic Al Kα source with a binding energy of 1486.6 eV and a beam size diameter of 100 μm.

### 2.4. Hydrotreating and co-hydroprocessing setup

The hydroconversion experiments conducted in this study are structured into three distinct sections. In the initial section, hexadecane and hydrolysis lignin were employed to assess the performance of the unsupported NiMoP catalyst under varied operating conditions (refer to Table 2, labeled as $HEP_0$ to $HEP_6$). This screening process was conducted during the first cycle of experimentation (see Fig. 1a). Moving on to the second section, multi-cycling studies were conducted. A consistent quantity of hydrolysis lignin was introduced into the lignin-oil blends obtained from the first cycle without the removal of spent catalyst and solids (referred to as cycle 2, Fig. 1b). This procedure was identically repeated for a third cycle (refer to Table 2, labeled as $HEP_7$ to $HEP_9$), as illustrated in Fig. 1b. Similarly, the third section involved single and multi-cycling experiments conducted with VGO as a representative petroleum oil feedstock (refer to Table 2, labeled as $HEP_{10}$ to $HEP_{17}$). For each section, reference and blank experiments were carried out. Reference experiments, conducted without lignin, served to remove the effects of thermal and catalytical hydrotreated and hydrocracked VGO and hexadecane for monomeric composition studies utilizing GCxGC analysis.

#### 2.4.1. Hydrotreating experiments

The experiments were conducted in a 450 mL Parr reactor. The processing feedstock, comprising 7.5 wt% hydrolysis lignin and 92.5 wt % petroleum intermediates, was employed. Catalyst loadings ranging from 5 to 20 wt% (based on the initial 5 g of dry lignin charged into the vessel at the start of the first cycle), pressures varying between 50–80 bar $H_2$, and temperatures ranging from 330 to 400°C were investigated. Typically, the reaction chamber was loaded with catalyst (0.25, 0.5, or 1 g) and 5 g of hydrolysis lignin in 67 g of the petroleum intermediate or solvent, as illustrated in Fig. 1a. Subsequently, the reactor was sealed, purged several times with $N_2$ gas to eliminate air, and then flushed with $H_2$ gas. Upon achieving leak tightness, the vessel was pressurized with 16–25 bar $H_2$ at room temperature (adjusted based on the expected pressure at the final reaction temperature) and heated to the designated reaction temperature while being stirred at 1200 rpm, with a heating rate of 5°C/min. The residence time was considered zero once the desired reaction pressure and temperature were reached. This entire procedure, described herein, is referred to as a single cycle (Fig. 1a).

**Table 2**
Catalytic hydrotreatment and co-hydroprocessing operational conditions.

| Experiments Notation | Operating Conditions $HL^a$–$T^b$–$P^c$–$t^d$–$W^e$ |
|---|---|
| *Hydrotreatment Lignin in hexadecane – single cycle* | |
| $HEP_0$ (Blank) | HL–400–80–5–$W_0$ |
| $HEP_1$ | HL–330–50–5–$W_5$ |
| $HEP_2$ | HL–400–50–5–$W_5$ |
| $HEP_3$ | HL–400–80–5–$W_5$ |
| $HEP_4$ | HL–400–80–5–$W_{10}$ |
| $HEP_5$ | HL–400–80–5–$W_{20}$ |
| $HEP_6$ | HL–400–80–12–$W_{20}$ |
| *Co-hydroprocessing lignin in Lignin-oil-C16 blends – multi-cycle* | |
| $HEP_7$ (Blank) | HL*–400–80–15–$W_0$ |
| $HEP_8$ | HL*–400–80–15–$W_5$ |
| $HEP_9$ | HL*–400–80–15–$W_{20}$ |
| *Hydrotreatment lignin in VGO – single cycle* | |
| $HEP_{10}$ (Blank) | HL–400–80–5–$W_0$ |
| $HEP_{11}$ | HL–400–80–5–$W_5$ |
| $HEP_{12}$ | HL–400–80–5–$W_{20}$ |
| $HEP_{13}$ (Blank) | HL**–400–80–15–$W_0$ |
| $HEP_{14}$ | HL**–400–80–15–$W_{20}$ |
| *Co-hydroprocessing lignin in Lignin-oil-VGO blends – multi-cycle* | |
| $HEP_{15}$ (Blank) | HL*–400–80–15–$W_0$ |
| $HEP_{16}$ | HL*–400–80–15–$W_5$ |
| $HEP_{17}$ | HL*–400–80–15–$W_{20}$ |

[a]Indicates Hydrolysis Lignin (HL), [b] Temperature reached (°C), [c] $H_2$ Pressure reached (bar), [d] residence time (h), [e] wt.% of catalyst charged based on 5g of dry lignin in a single cycle. 5g of lignin is used for cycle 1. * indicates 3 cycles per experiment with 5g lignin for cycle 1 and 2.5 g for cycles 2 and 3. ** 10 g total added lignin. HEP7 to HEP9 and HEP15 to HEP17, contains 3 cycles for each experiment.

#### 2.4.2. Multicycle co-hydrotreating experiments

In cycle 2, the lignin-oil blend obtained from cycle 1 served as the solvent for further lignin hydroprocessing, as illustrated in Fig. 1b. During this cycle, 2.5 g of fresh lignin feedstock (~ 4 wt%) was added to the produced lignin-oil blend from cycle 1, without removing the products and spent catalyst. Subsequently, in the last cycle (cycle 3), 2.5 g of fresh lignin was added to the product of cycle 2, following the procedure outlined in Fig. 1b. Throughout this process, the produced lignin-oil blend and spent catalyst were successively reused. These multicycle experiments were conducted at 400°C and approximately 80 bar $H_2$, while maintaining stirring at 1200 rpm. Upon completion of the reaction, the reactor was cooled using cold water. The resulting products, comprising gas, liquid bio-oil, unreacted lignin, and solid char, were then separated, and analyzed in accordance with the product recovery protocol outlined in our recent study [37].

### 2.5. Products analysis

Mass balance calculations were conducted using measurements obtained from a combination of collected liquids, solids, and the gas phase following each experiment. The final pressure post-experiment was recorded at room temperature to facilitate the calculation of hydrogen consumption, considering the gas as ideal and based on its composition [42,43]. The gaseous products were subsequently collected in Tedlar bags.

The lignin-oil blend product was recovered from solids via filtration and labelled as lignin oil. Next, the vessel was cleaned with acetone. The resulting product fraction was then filtered and identified as the acetone-soluble phase. Following this, the solid phase, comprising char, unconverted lignin, and catalyst, underwent further rinsing with acetone to enable liquid–liquid extraction. The non-converted lignin was quantified by suspending the solid phase in DMSO and vigorously mixing for 24 h at room temperature. The remaining solids, post-filtration, were washed with acetone and dried. The weight of dried solids, after subtracting the spent catalyst, was considered to be the weight of char. The organic constituents of the lignin oil were analyzed and quantified using a comprehensive two-dimensional gas chromatography (GCxGC) system, featuring an Agilent 7890B coupled with a Mass Spectrometer (5977A MSD). The GCxGC setup is enhanced with a closed cycle cryogenic jet modulation (ZX2 Model) from Zoex Corporation. For product separation, two columns were employed: a moderate polar VF1701ms column (30 m × 0.25 mm × 0.25 μm) served as the first dimension, followed by a nonpolar DB-5 MS UI column (3 m × 0.15 mm × 0.15 μm) in the second dimension. The injector and MS interface were both maintained at 250 °C. A column flow rate of 0.8 NmL/min was utilized. The temperature program for the oven comprised an initial temperature of 40 °C, held for 1 min, followed by a ramp to 280 °C at 3 °C/min. Notably, the relative standard deviations in the first and second dimensions, as well as the peak volume, were less than 0.3 %.

Simulated Distillation using TGA (SimDist TGA) was carried out using a TGA/DSC 3 + Star analyzer (Mettler Toledo, Switzerland). In this method, a sample is heated gradually from 30 °C to 750 °C at a rate of 50 °C/min under $N_2$ flow of 50 NmL/min. As the temperature increases, the components of the sample vaporize or decompose at different temperatures according to their boiling points. The rate of mass loss is recorded as a function of temperature, and from this data, the boiling point distribution of the sample can be simulated and controlled

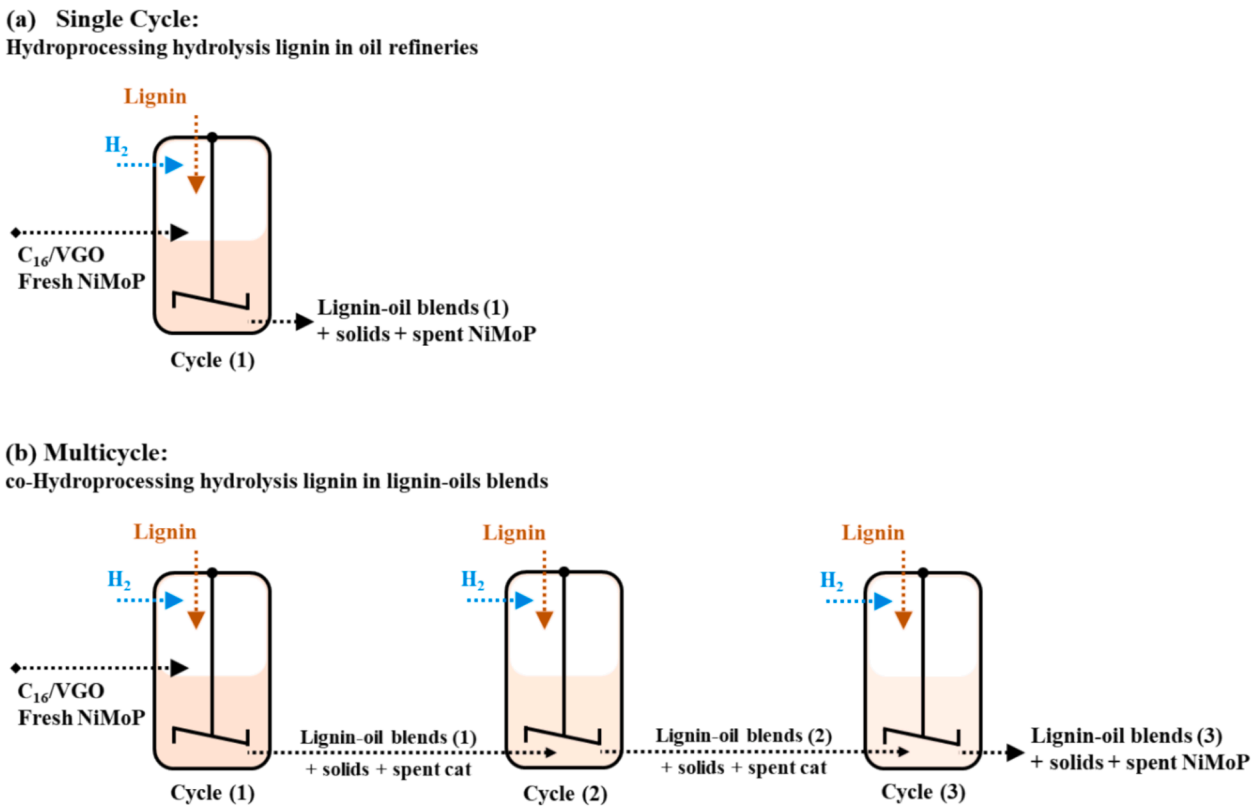


**Fig. 1.** Schematic representation of the hydrotreatment experiment procedure (a) and multi-cycling of lignin-oil blends with addition of hydrolysis lignin (b).

using petroleum reference such as VGO. The gaseous products generated during the hydroconversion of lignin were analyzed using gas chromatography with a thermal conductivity detector (GC-TCD, 450-GC, Varian). Components such as CO, $CO_2$, $CH_4$, and $C_2$ + light hydrocarbons were identified and quantified using a GS-GASPRO column (30 m, 0.32 mm). The CHNS-O content in the feedstocks and lignin oils were determined using a Vario MICRO cube analyzer. The amount of oxygen was assessed by the difference from the CHNS content. Additionally, the total water content in organic samples was determined via volumetric Karl Fischer titration, utilizing a Metrohm Titrino 807. All laboratory analyses were conducted in duplicate to ensure accuracy and reproducibility. For further details, refer to our previous work [37].

### 2.6. Data processing

Equations (1)–(5) were used to determine the conversion, mass balance, the yields of char, gas and monomers.

$$\text{Conversion (wt.\%)} = \frac{\text{lignin feed (g)} - \text{non} - \text{converted lignin (g)}}{\text{lignin feed (g)}} \times 100 \quad (1)$$

$$\text{Mass balance (wt.\%)} = \frac{\sum \text{products (g)}}{\text{lignin feed (g)}} \times 100 \quad (2)$$

$$\text{Char yield (wt.\%)} = \frac{(\text{total solid fraction (g)}) - (\text{unconverted lignin (g)} + \text{catalyst (g)})}{\text{lignin feed (g)}} \times 100 \quad (3)$$

**Table 3**
Catalyst textural properties, metal content and total acidity uptake.

| Catalyst | Textural properties | | | Chemical composition (wt.%)* | | | $NH_3$-TPD uptake |
|---|---|---|---|---|---|---|---|
| | $S_{BET}$ [a] | $V_{mes}$ [b] | $d_{BJH}$ [c] | Ni | Mo | P | (μmol/g) |
| NiMoP | 196.3 | 0.2 | 4.3 | 86.6 | 9.1 | 4.3 | 457.96 |

[a] $S_{BET}$: Surface area **($m^2 \cdot g^{-1}$).** [b] The total pore volume **($cm^3 \cdot g^{-1}$)** was measured at a relative pressure of 0.99. [c] Mesopore diameter **(nm)** was determined using the BJH method. *ICP-MS determined.

$$\text{Gas yield (wt.\%)} = \frac{\text{amount of gas (g)}}{\text{lignin feed (g)}} \times 100 \quad (4)$$

$$\text{Monomer yield (wt.\%)} = \frac{\text{monomer (g)}}{\text{lignin feed (g)}} \times 100 \quad (5)$$

The deoxygenation degree (De-O), hydrogen consumption and energy recovery were calculated as follows:

$$\text{De} - \text{O (\%)} = \left(1 - \frac{\text{Oxygen content in lignin oil}}{\text{Oxygen content in lignin}}\right) \times 100 \quad (6)$$

$$\text{Hydrogen consumption} = \frac{\text{weight of gas per initial lignin feed x concentration of hydrogen / 100}}{\text{Molar mass of hydrogen}} \times 1000 \quad (7)$$

$$\text{Energy recovery} = \frac{\text{Lignin} - \text{oil yield x its Higher Heating Value}}{\text{Heating Value of hydrolysis lignin}} \quad (8)$$

## 3. Results and discussions

### 3.1. Microstructure analysis of NiMoP catalyst

The textural properties and chemical composition of the catalyst are summarized in Table 3. $N_2$ physisorption data shows that the surface area is high compared to other unsupported NiMoP catalysts [44] and reached 196 $m^2/g$. The synthesized catalysts show the type-IV isotherm, exhibiting their ordered *meso*-structure (Fig. 2a and 2b). The hysteresis loop of the NiMoP isotherm is of $H_4$ type, which is often found for aggregated crystals of zeolites, micro-mesoporous carbons [45]. In addition, the pore size distribution corresponds well with those of the template used. The unsupported NiMoP catalyst also showed a narrow pore size distribution at around 4.3 nm with a pore volume of 0.2 $cm^3 g^{-1}$.

This implies that the unsupported catalyst possessed open pores and large surface areas, which could enable the diffusion of reactants in the mesoporous pores. The measurement of Ni, Mo, and P content by ICP-OES gave values of Ni = 86.6 wt%, Mo = 9.1 wt%, and P = 4.3 wt%. These values are close to their nominal values. The presence of $SiO_2$-based material in the unsupported catalysts was also investigated and ICP confirmed the absence of template, indicating successful template removal. Moreover, the absence of silica was confirmed using XRD. The XRD spectra of the unsupported NiMoP catalyst in the present investigation is shown in Fig. 2c. The NiMoP fabricated via the hard SBA template reveals a characteristic peak of the β-$NiMoO_4$ phase at 2θ = 26.4°. A nickel phosphide phase was also detected, attributed to phosphides. According to the literature, nickel phosphide catalysts ($Ni_2P$-based) has attracted attention due to their reactivity and tolerance in HDO, hydrodesulfurization (HDS), as well as hydrodenitrogenation (HDN) processes [46,47]. Catalytic $Ni_2P$-based materials appear to be a promising catalytic system that can meet the HDO process requirements, such as high activity, non-sulfided nature and low-cost catalysts [46,47]. The thermal decomposition of the unsupported NiMoP was evaluated by TGA (Fig. 2d). The weight loss curve and its derivative for the thermal decomposition of the unsupported NiMoP catalyst are shown within the temperature range 30 to 800°C. A mass loss of 3.2 wt% in net weight, up to 400°C occurred.

To explore the acidic properties of the unsupported NiMoP, the ammonia TPD technique was employed, as shown in Fig. 3a. Two desorption peaks of ammonia centered at 250 and 500 °C were observed, with a total quantity of acid sites equaling 457.96 μmol/g (Table 3). The first desorption peak around 250 °C corresponds to sites with the

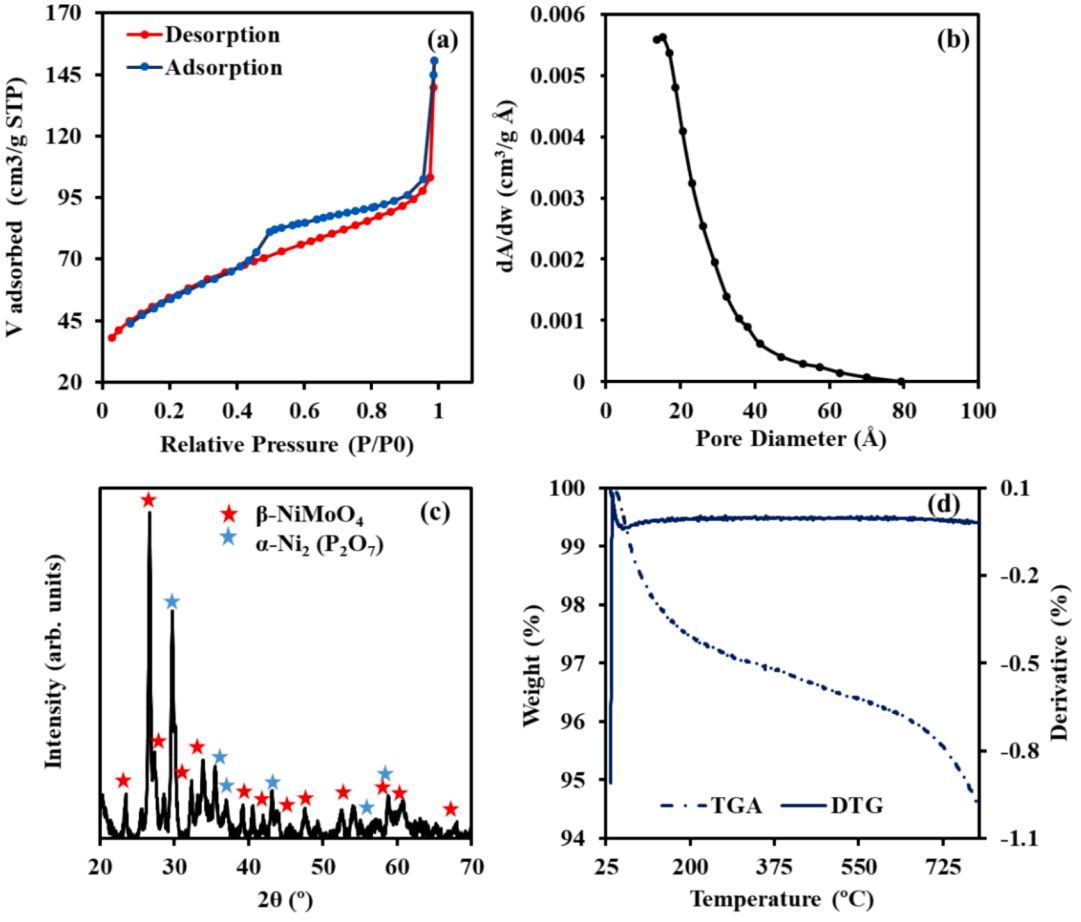


**Fig. 2.** BET adsorption and desorption (a) pore diameter (b) XRD pattern (c) and TGA/DTG (d) of the NiMoP catalyst.

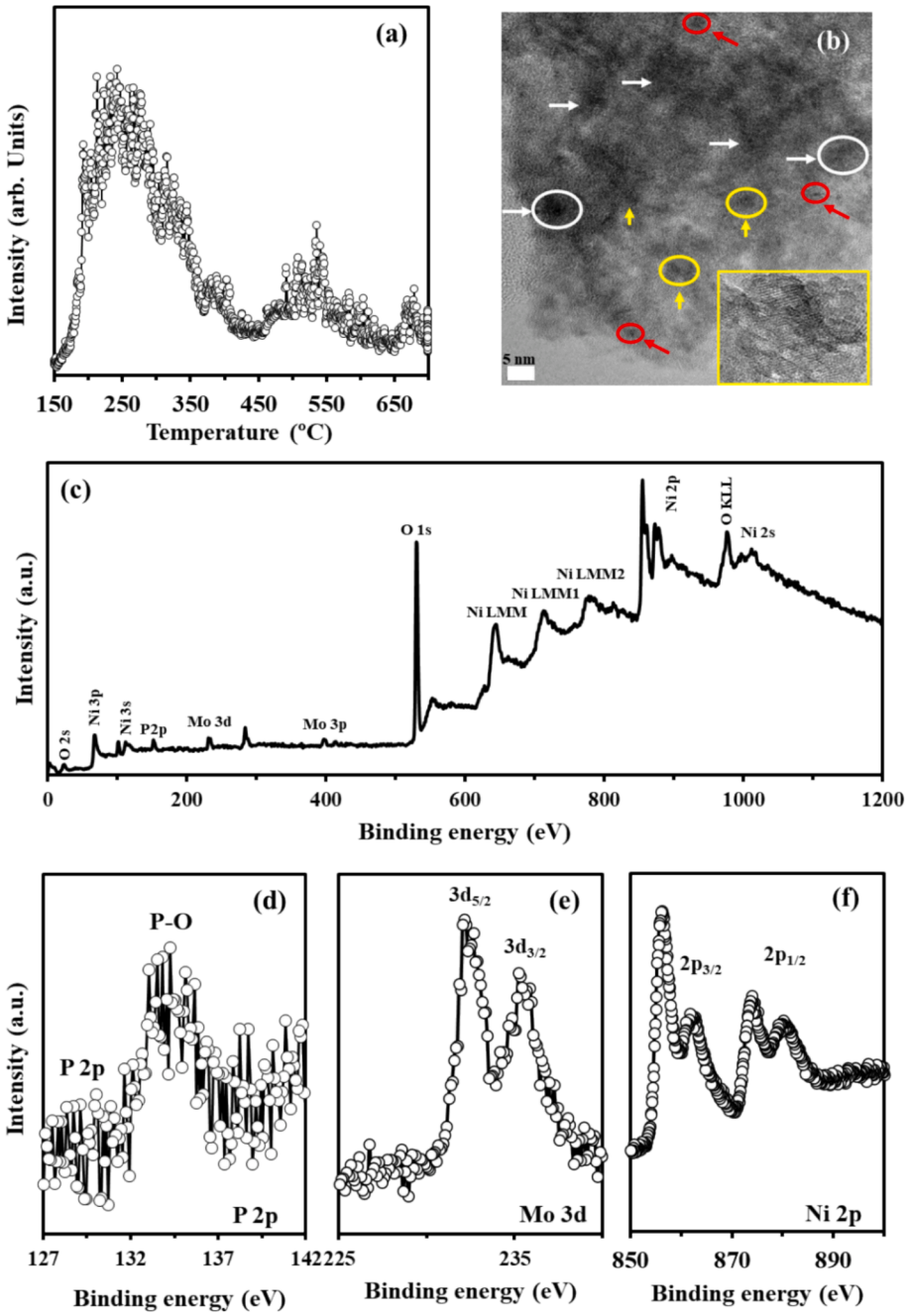


**Fig. 3.** $NH_3$-TPD curve (a) HRTEM images (b) XPS spectra (d-g) of the unsupported phosphided NiMoP powder.

weakest acidity, responsible for physisorbed and chemisorbed ammonia, constituting 70 % of the total acidity. The second desorption peak at 500 °C was assigned to moderate-strength acid sites. According to the literature, $PO_x$ groups are responsible for the weak Brønsted acidity of NiMoP catalysts [48]. TEM analysis of NiMoP shows large aggregates, while the TEM image clearly depicts the nanoparticulate composition of the catalyst (Fig. 3b). The spherical nanoparticles with an average size of 8–10 nm are found to be crystalline. A distinct difference in crystal indices could be observed among different spherical nanoparticles, as typical lattice fringes are detected (insert in Fig. 3b). The bimetallic alloy nature of the NiMoP catalyst was further confirmed by the XRD pattern of NiMo/Ni-P.

XPS spectra were also analyzed to investigate the electronic interaction, chemical composition, and valence states of the material. The comprehensive survey spectrum in Fig. 3c distinctly reveals the presence of Ni, Mo, P and O. Fig. 3d depicts the XPS spectra of P elements, with peaks located at 133.98 eV attributed to oxidized P species ($PO_4^{3-}$) due to air exposure [49]. An additional small peak at 129.85 eV can be assigned to P 2p. The Mo 3d spectrum (Fig. 3e) displays two peaks at 232.3 and 234.2 eV, corresponding to Mo $3d_{5/2}$ and Mo $3d_{3/2}$, indicative of $Mo^{6+}$ characteristics. Furthermore, the significant M−O−M peaks at 530.8 eV denote the lattice oxygen in NiMoP [50]. Fig. 3f illustrates the Ni 2p spectrum, revealing well-defined two spin–orbit doublets of Ni $2p_{3/2}$ (856.4 eV) and Ni $2p_{1/2}$ (873.9 eV), accompanied by two satellite peaks around 862.8 and 880.6 eV. The observed gap of 17.8 eV between the main peaks of Ni $2p_{3/2}$ and Ni $2p_{1/2}$ is 17.8 eV concurs with the characteristic of $Ni^{2+}$. These findings align reasonably well with the XRD results.

**Table 4**
Summary of thermal and catalytic hydrotreatment of lignin with hexadecane.

| Entry | Operating Conditions | Lignin Conv. (Wt.%) | Lignin Oil (Wt.%) | Gas (Wt.%) | Char (Wt.%) | Water (Wt.%) | $H_2$ Consumption* (mmol/g lignin) |
|---|---|---|---|---|---|---|---|
| *HDO Lignin in hexadecane**- single cycle* | | | | | | | |
| $HEP_0$ | HL–400–80–5–$W_0$ | 96.0 | 56.4 | 0.7 | 38.6 | 1.5 | 0.3 |
| $HEP_1$ | HL–330–50–5–$W_5$ | 94.9 | 56.7 | 1.1 | 35.9 | 1.3 | 1.9 |
| $HEP_2$ | HL–400–50–5–$W_5$ | 92.9 | 74.2 | 2.0 | 14.5 | 2.2 | 5.8 |
| $HEP_3$ | HL–400–80–5–$W_5$ | 95.6 | 77.0 | 2.8 | 12.9 | 2.3 | 9.0 |
| $HEP_4$ | HL–400–80–5–$W_{10}$ | 93.4 | 79.0 | 1.6 | 10.0 | 2.8 | 12.1 |
| $HEP_5$ | HL–400–80–5–$W_{20}$ | 95.7 | 84.6 | 1.5 | 6.7 | 2.9 | 15.2 |
| $HEP_6$ | HL–400–80–12–$W_{20}$ | 98.2 | 87.8 | 2.8 | 4.6 | 3.0 | 20.1 |

* See equation (7) **Hydrolysis lignin-Temperature in °C-Pressure in bar-time in hour-catalyst loading in %.

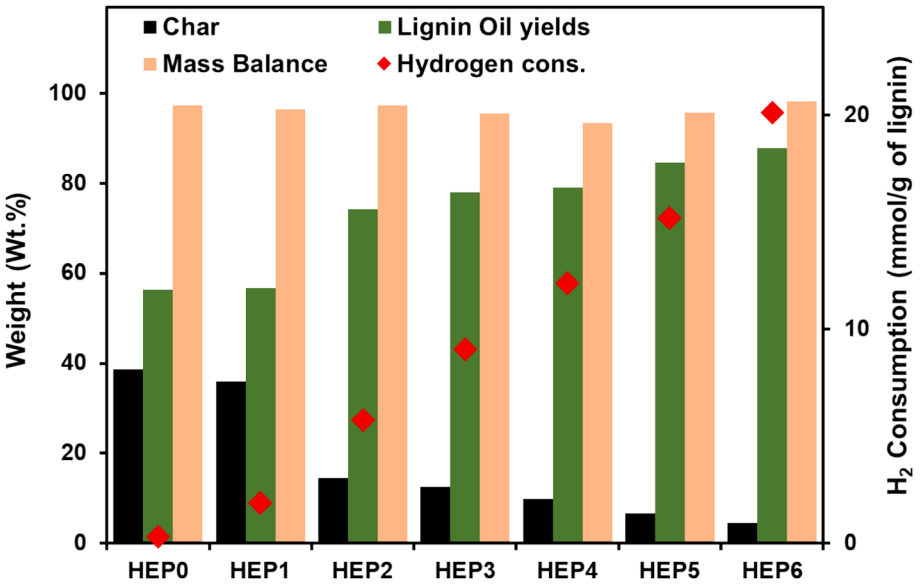


**Fig. 4.** Mass balance, lignin-oil, char yields and $H_2$ consumption of lignin-oils from hydrolysis lignin hydrotreatment in hexadecane.

### 3.2. Hydrotreating lignin in paraffinic oil

The chemical and structural characterization of hydrolysis lignin residue has been extensively detailed in our recent study [37]. To assess the catalytic performance of hydrolysis lignin residue, we conducted a series of experiments under various reaction conditions, as outlined in Table 2 (Hydrotreatment Lignin in hexadecane – single cycle 1). These experiments involves varying parameters such as temperature, pressure, reaction time and catalyst loading. The resulting product distribution from hydrolysis lignin hydroconversion in hexadecane is summarized in Table 4. The products are categorized into five parts: lignin oil, non-condensable gas, char, water yields and hydrogen consumption. The overall mass balance from the product distributions ranged from 93 to 98 wt% excluding hydrogen consumption (Table 4 and Fig. 4).

The hydrothermal reaction of lignin in hexadecane without catalyst was conducted at 400 °C and 80 bar $H_2$ pressure, (HL-400–80-5-$W_0$). Among all the catalytic hydrothermal experiments, this resulted in the highest char weight yield, with 38.6 wt% char (Table 4). Introducing a 5 wt% catalyst ($HEP_3$: HL–400–80–5–$W_5$) significantly reduced the char amount to 12.9 %. However, lowering the reaction pressure and temperature while maintaining a 5 wt% catalyst loading ($HEP_1$: HL-330–50-5-$W_5$) led to a higher char yield of 35.9 %. These results were similar to those obtained without a catalyst at higher temperature and pressure (HL-400–80-5-$W_0$), albeit with a slight increase in hydrogen consumption, which might impact the yields of monomeric products by increasing the isomeric hydrocarbons and ketones/alcohols, as discussed later. The product distribution results reported in Table 4 illustrate the decline in char yields as temperature, pressure and catalyst loading increased, accompanied by a proportional increase in hydrogen consumption and lignin-oil yields.

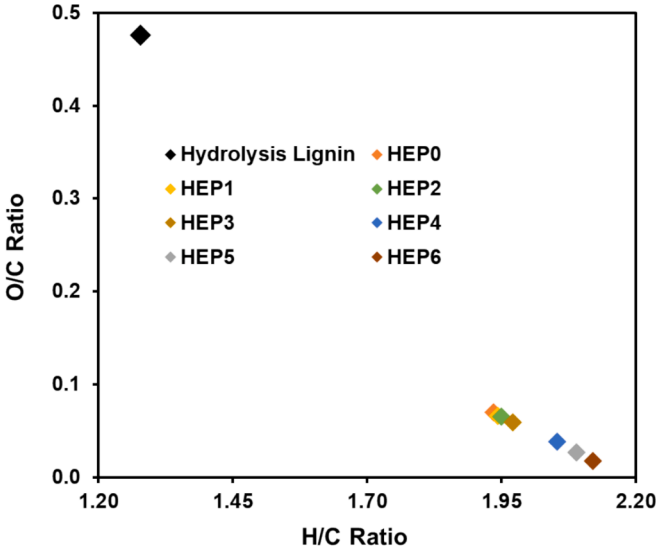


**Fig. 5.** Krevelen diagram of lignin-oils from hydrolysis lignin hydrotreatment in hexadecane.

These results are also clearly illustrated in Fig. 4. A low char yield of 6.7 wt% was achieved with 20 wt% of catalyst loading under the conditions of 400 °C and 80 bar, followed by a 12.9 wt% char yield with 5

wt% catalyst loading ($HEP_3$). Extending the reaction time from 5 to 12 h in $HEP_6$ resulted in the highest lignin-oil yield of 87.8 wt%, accompanied by the highest hydrogen consumption and the lowest char yield of 4.6 wt%. Additionally, the soluble solid (referred to as unreacted lignin) decreased from 4.3 to 1.9 wt% with an increase in reaction time from 5 to 12 h, demonstrating an increased lignin conversion (Table 4). These observations suggest a positive catalytic effect on lignin-oil yields with sufficiently elevated temperature and pressure. Based on these findings, there is an opportunity to enhance the yield of stabilized compounds while suppressing char formation and condensation reactions at relatively higher hydrogen pressure [51].

The elemental composition of the lignin-oil products is crucial for understanding the varying reaction chemistry under different conditions. The catalytic hydrotreatment of hydrolysis lignin (experiments $HEP_1$ to $HEP_6$) exhibited deeper deoxygenation performance compared to thermal hydrotreatment ($HEP_0$), often resulting in higher lignin-oil yields (Table 4). Fig. 5 illustrates the changes in O/C and H/C atomic ratios of the lignin-oil obtained with the unsupported NiMoP. For instance, the O/C atomic ratio shows a clear reduction with increasing reaction time ($HEP_5$ to $HEP_6$), while the H/C ratio increased. Consequently, the hydrogen consumption increased to 20.1 mmol/g, as displayed in Fig. 4a. Under $HEP_5$ operating conditions (HL-400–80-5-$W_5$), the O/C atomic ratio decreased by 68 %, whereas the H/C atomic ratio increased by 24 % compared to $HEP_1$: HL-330–50-5-$W_5$. Since the O/C ratio is correlated with hydrogen consumption, these results suggest that higher hydrogen consumption (from 1.9 to 15.2 mmol/g) at higher temperature, pressure and catalyst loading influenced the lignin-oil yields by affecting the activity for breaking O–H, C—O, C–C, and C–H bonds. This has been previously confirmed using model compounds over NiMo/MoP/$Ni_2P$ [46,47]. The authors claimed that the active site of $Ni_2P$ catalysts is composed of threefold hollow Ni and P sites which lead to adsorption of H or OH groups.

In this study, hydrogen utilization efficiency was assessed by calculating the bio-oil yield per mmol of hydrogen consumed during the hydroprocessing of lignin with hexadecane. The analysis indicates that as catalyst loading increases, hydrogen consumption rises, accompanied by an increase in bio-oil yield. However, hydrogen utilization efficiency, defined as the bio-oil yield (in %) per mmol of hydrogen, tends to decrease with higher catalyst loadings. For the single-stage hydroprocessing of hexadecane, the hydrogen utilization efficiency was highest for the blank (HEP0), at 9.6 % bio-oil per mmol of hydrogen, with a relatively low bio-oil yield of 49.2 %. As catalyst loadings increased, the bio-oil yield significantly improved (77.9 % for 5 % catalyst and 87.8 % for 20 % catalyst), but the hydrogen utilization efficiency decreased to 4.1 %/mmol $H_2$ and 3.3 %/mmol $H_2$, respectively.

**Table 5**
Monomer yields and distillates distribution for the lignin-oils.

| Properties | $HEP_0$ | $HEP_1$ | $HEP_2$ | $HEP_3$ | $HEP_4$ | $HEP_5$ | $HEP_6$ |
|---|---|---|---|---|---|---|---|
| total | 32.7 | 45.5 | 60.7 | 75.6 | 81.0 | 84.3 | 89.8 |
| light alkanes/ alkenes (< $C_{10}$) | 3.0 | 4.8 | 5.0 | 9.2 | 9.6 | 11.0 | 14.1 |
| heavy alkanes/ alkenes (>$C_{10}$) | 5.0 | 9.2 | 12.0 | 14.0 | 15.7 | 20.1 | 24.1 |
| cycloalkanes | 0.5 | 3.9 | 8.2 | 8.3 | 9.0 | 10.1 | 11.1 |
| aromatics | 11.3 | 11.0 | 12.4 | 14.1 | 14.2 | 16.0 | 17.9 |
| ketones/alcohols | 2.0 | 5.4 | 7.1 | 11.0 | 13.0 | 14.1 | 15.1 |
| Alkylated phenolics | 11.9 | 11.2 | 16.0 | 19.0 | 19.5 | 13.1 | 7.5 |
| naphtha range (wt. %, IBP-177 °C) | 3.6 | 3.8 | 6.4 | 8.6 | 10.3 | 13.5 | 17.6 |
| distillate range (wt. %, 177–343 °C) | 88.3 | 94.5 | 93.6 | 91.4 | 89.7 | 86.5 | 82.4 |
| heavy oil range (wt. %, 343–524 °C) | 8.1 | 1.5 | 0.0 | 0.0 | 0.0 | 0.0 | 0.0 |
| residue (wt.%, > 524 °C) | 0 | 0 | 0.0 | 0.0 | 0.0 | 0.0 | 0.0 |

Similarly, in the multicycle hydroprocessing using hexadecane, higher catalyst loadings resulted in higher bio-oil yields (93.2 % for 20 % catalyst), but hydrogen utilization efficiency decreased from 5.0 %/mmol $H_2$ for the blank (HEP7) to 2.9 %/mmol $H_2$ for the 20 % catalyst (HEP9).

Table 5 presents the GCxGC detectable monomeric components of the lignin-oils resulting from the hydrocatalytic treatment of the hydrolysis lignin in hexadecane (single cycle, Fig. 1a). As the temperature and pressure increased from $HEP_1$ to $HEP_3$ (300 to 400 °C and 50 to 80 bar), the monomer yield significantly increased from 45.5 to 75.6 wt%, accompanied by higher hydrogen consumption (1.9 to 9.0 mmol/g of lignin). Remarkably, char and unreacted lignin residue yields (Table 4) were also notably reduced in all of these cases. Under our optimum temperature and pressure conditions (400 °C, 80 bar and 5 h) with 20 wt % catalyst loading, a monomer yield of 84.3 wt% was obtained ($HEP_5$ in Table 5), of which approximately 27.2 % were oxygenated compounds. This highlights the high deoxygenation capacity provided by the catalyst, as confirmed by analyzing the lignin residue using elemental analysis. A similar trend was observed in the hydrodeoxygenation of hydrolysis lignin using the NiMoS catalyst [37].

The predominant chemical compounds in all catalytic experiments are isomeric hydrocarbons, constituting a fraction ranging between 8.5 and 41.2 wt% of the liquid product ($HEP_0$ to $HEP_5$). Notably, heavy aliphatic hydrocarbons (> $C_{10}$) were the most abundant, with yields ranging from 5.0 to 20.1 wt%, and their production increased progressively with hydrogen consumption (0.3 to 15.2 mmol/g) towards the optimum operating conditions at 400 °C, 80 bar, 20 wt% catalyst loading. The yield of aromatic hydrocarbons remained stable in runs with varying catalyst loading ($HEP_3$, $HEP_4$ and $HEP_5$). Conversely, the lower yields of alkylated phenolics ($HEP_6$: 7.5 wt%) are likely attributed to high rates of dealkylation, demethoxylation, and decarboxylation reactions, leading to increased alcohol, ketone, and acid yields. A higher ratio of alcohols and ketones to alkylated phenolics indicates a greater extent of alkylation and/or transalkylation reactions. Compared to the non-catalytic hydrogenation experiment ($HEP_0$), NiMoP had a more pronounced impact on aliphatic hydrocarbons and cycloalkanes rather than aromatics. This suggests that in reactions with NiMoP, cellulose units present in hydrolysis lignin undergo partial hydrodeoxygenation to form oxygenated compounds and subsequently hydrocarbons. This is consistent with the results obtained from the catalytic hydrogenation of cellulose to hydrocarbons using hexadecane as a solvent [52]. Hydrocarbon products (<C10, >C10, and cycloalkanes) are ideally suited for converting cellulose in hydrolysis lignin to isomeric hydrocarbons, yielding high carbon content. However, in the reactions with NiMoS [37], the yield of aliphatic hydrocarbons was threefold lower than with NiMoP. Despite the complex composition of lignin, the unique characteristics of the NiMoP catalyst, particularly the $Ni_2P$ phase, significantly influence the product distribution of monomers, which differs from that observed with the NiMoS catalyst [37].

To ascertain the boiling point distribution of the produced lignin-oil blends from hydrotreated lignin in hexadecane, a simulated distillation method was conducted using TGA, with the results summarized in Table 5. Note, reference experiments were performed to remove the solvent effect. The boiling points of the major components of the obtained lignin oils fell within the temperature range of 100°C to 200 °C, akin to the naphtha fraction (< 177°C), and distillate range components (177–343 °C). Conversely, higher-boiling components, characteristic of heavy oil with boiling points > 343°C, were observed in the non-catalytic and low pressure and temperature experiments ($HEP_0$ to $HEP_1$). These findings suggest a less hydrogenation occurred, in line with the lower hydrogen consumption observed under these conditions. Notably, these high-boiling products were undetectable by GCxGC ($HEP_0$: 8.1 and $HEP_1$: 1.5 wt%), yet they significantly impact the composition and quality of the resulting lignin-oil.

Comparatively, the variation in NiMoP at 400 °C and 80 bar conditions ($HEP_3$, $HEP_4$, $HEP_5$) influenced the boiling point distribution of the

lignin-oil. Particularly, the content of the naphtha was further enhanced, but not highly impacted by the hydrotreatment severity as consistently found by Gueudré *et al.* [53], Alvares-Majmutov *et al.* [29]. and Melin *et al.* [26]. These results suggest that the increased naphtha/distillates ratios were accelerated by dealkylation, demethoxylation, and decarboxylation of alkylated phenolics, leading to the formation of cycloalkanes, aromatics, and aliphatic hydrocarbons, significantly augmented with hydrogen consumption (Tables 4 and 5). Especially, when extending the reaction time to 12 h, the naphtha component content reached 17.6 %, while simultaneously, the distillate content decreased from 86.5 to 82.4 % for $HEP_6$. This observation suggests that NiMoP effectively promotes the hydrocracking of additional macromolecules (e.g., naphthalenes benzene structures) and further deoxygenation of lignin-oil components towards lighter end products, contrasting with our previous study using the NiMoS catalyst [37].

### 3.3. Co-hydroprocessing of hydrolysis lignin in lignin-oil-C16 blends

In this study, we conducted experiments using lignin-oil blends obtained from hydroprocessing lignin with hexadecane (single cycle). Subsequently, this product was used as a solvent for co-hydroprocessing with an additional amount of hydrolysis lignin without removing the produced solids and spent catalyst (Fig. 1b). The primary objective was to evaluate the impact of co-hydroprocessing lignin with lignin-oil blends while gradually increasing the sustainable component in the product. Importantly, the lignin-oil blend is expected to provide further insights into the catalyst's cracking efficiency regarding downstream operational opportunities. To scrutinize the multi-cycling use of the NiMo phosphided catalyst and gain a deeper understanding of its performance with different catalyst loadings (Fig. 6a), the product distributions were analyzed to examine the upgrading of the lignin-oil blends in more detail.

According to Fig. 6a, the multicycle experiments of lignin-oil blends initiated with hexadecane over increasing NiMoP loadings ($HEP_7$ to $HEP_9$) resulted in a significant increase in lignin-oil yield, reaching up to 93.2 wt%, with only 5.0 wt% of char formation and reasonable gas yields of up to 6.9 wt%. In comparison, without NiMoP ($HEP_7$), the char yield was significantly higher at 42.0 wt% and resulting in a lower lignin-oil yield of 49.2 wt% compared to the single-cycle experiment ($HEP_0$, Fig. 4). Fig. 6b also displays the Van Krevelen diagram of the lignin-oil blends co-processed in the multicycle scheme with lignin. Due to its much lower lignin-oil and higher char yields in the recirculation of lignin without catalyst ($HEP_7$), the atomic O/C ratio was highly

**Table 6**
Monomer yields and boiling-point distribution for multicycling of lignin-oil blends initiated with hexadecane as a function of NiMoP catalyst loadings of 0, 5 and 20 wt%.

| Properties | $HEP_7$ | $HEP_8$ | $HEP_9$ |
|---|---|---|---|
| *SimDist TGA Recirculated* | | | |
| naphtha range (wt.%, IBP-177 °C) | 5.5 | 16.8 | 41.0 |
| middle distillate range (wt.%, 177–343 °C) | 92.5 | 83.2 | 58.0 |
| heavy oil range (wt.%, 343–524 °C) | 2.0 | 0.0 | 0.0 |
| residue (wt.%, > 524 °C) | 0 | 0 | 0.0 |
| *monomer distribution (GCxGC)* | | | |
| total | 47.5 | 74.2 | 92.2 |
| light alkanes/alkenes (< C10) | 4.6 | 19.5 | 17.0 |
| heavy alkanes/alkenes (>C10) | 11.0 | 21.0 | 27.0 |
| cycloalkanes | 1.2 | 6.4 | 9.9 |
| aromatics | 6.2 | 8.0 | 9.5 |
| ketones/alcohols | 13.0 | 12.9 | 18.9 |
| alkylated phenolics | 11.5 | 6.4 | 9.9 |

enriched. This result indicates that hydrogenation of the lignin-oil blend was less likely to occur, and the yield of deoxygenated oil products was therefore sacrificed. In contrast, the atomic H/C of that with NiMoP increased as a function of catalyst loading ($HEP_8$ and $HEP_9$). This is in line with the increase in oil products and atomic H/C ratio and the decrease in char and O/C ratio, respectively. As a result, the consumption of hydrogen was about eightfold higher with NiMoP than without NiMoP. This aligns with the high yield of deoxygenated products, reaching 82.9 wt% within the lignin-oil product, of which approximately 44.0 wt% were aliphatic hydrocarbons for $HEP_9$. Despite higher consumption of hydrogen in the multicycle co-hydroprocessing, the elemental analysis results in Fig. 6b indicate an increase in oxygen content and a decrease in carbon compared to the single-cycle experiments (Fig. 4 and Table 5 for $HEP_0$, $HEP_3$ and $HEP_5$). These results suggest that more hydrogen consumption or limited blending is required to catalytically produce high-quality liquid fuel from the produced lignin-oil blends [54]. The multicycling of lignin-oil blends also revealed discernible differences in boiling point distributions, as shown in Table 6. The catalytic multicycle processing yielded a higher distillation profile, particularly with a high naphtha fraction for $HEP_9$. This indicates that recycling the lignin-oil blend with a high catalyst loading was conducive to enhancing the light end content of the lignin oil via hydrocracking reactions [13]. Interestingly, the naphtha fractions showed considerably higher yields for the lignin-oil recirculation

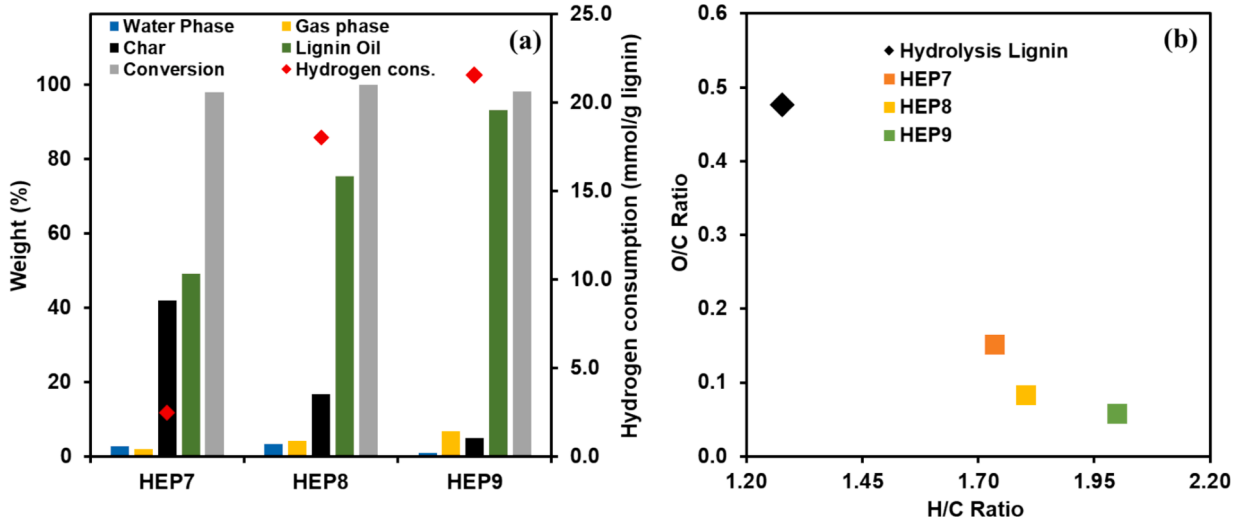


**Fig. 6.** Blank and catalytic multicycle hydrotreatments of lignin-oil blends initiated with hexadecane as a function of NiMoP catalyst loadings 0, 5 and 20 wt% (a) product distribution; (b) Van Krevelen diagram from elemental analysis of the lignin oils.

experiments ($HEP_8$: 16.8 wt% to $HEP_9$: 41.0 wt%) compared to their single-cycle counterparts (Table 5 for $HEP_3$: 8.6 wt% and $HEP_5$: 13.5 wt %).

The product compositions from catalytic multicycle co-hydroprocessing ($HEP_9$: HL 5 g + 2.5 g + 2.5 g–400–80–15–$W_{20}$) and single hydroprocessing ($HEP_6$: HL 5 g–400–80–12–$W_{20}$) can be compared, where with multicycling 100 % higher lignin feed is co-hydroprocessed with only 25 % longer residence time. The results were favorable for the recirculation process, as a higher lignin-oil yield was obtained ($HEP_9$: 93.2 vs. $HEP_6$: 87.8 wt%). However, the multi-cycling lignin-oil contains more oxygenated compounds, as displayed in Fig. 6a. Apart from lignin-oil yield, the char yields ($HEP_9$: 5.0 vs. $HEP_6$: 4.6) and hydrogen consumption ($HEP_9$: 21.5 vs. $HEP_6$: 20.1 mmol/g of lignin) were similar for both hydroprocessing. An additional difference between the single and multicycling processes is that with multicycling, after each cycle, the product gas is exhausted and replaced with fresh hydrogen. So, these results suggest that a higher hydrogen partial pressure is advantageous to enhance hydrogen solubility in the lignin-oil blends, allowing more hydrogen transfer to catalyst surfaces and the highly reactive compounds, as mentioned above. Evidently, the GCxGC analysis (Table 6) demonstrated that with the multi-cycling process ($HEP_9$), the yield of phenolic compounds increased in the product oil which resulted in lowering the cycloalkanes and aromatics compared to the single-cycle process ($HEP_6$, Table 5). Remarkably, further aromatization slightly enhanced ($HEP_7$ to $HEP_9$), as the yields of phenolics decreased, indicating that the co-processing over NiMoP using hexadecane as a solvent tends to enhance the hydrocracking activity rather than alkylation reactions. This result was consistently observed in the single cycle experiments ($HEP_5$ to $HEP_6$) when increasing the reaction time to 12 h. This also was confirmed for $Ni_2P$/HZSM-5 catalysts, and ascribed to the presence of strong acid sites, which promote hydrocracking and isomerization reactions [55]. Another remarkable hypothesis is that the amount of water strongly affects the maximum light alkanes/alkenes (C < 10) yield (see $HEP_8$). This value depends on the choice of the organic phase, as demonstrated by [32], where they observed cellulose to alkane conversion in a fossil naphtha/water system over a Ru supported on carbon catalyst, achieving complete cellulose conversion with efficiencies of 76 mol% C for petroleum ether (C5-C6) and 68 mol% C for petrol (C5-C12), while maintaining a similar product distribution of bio-based products between the two solvents, although a notable difference in carbon efficiency was observed.

### 3.4. Hydrotreating of hydrolysis lignin in VGO and multicycling in lignin-oil blends

Experiments discussed in this section involved hydroprocessing hydrolysis lignin alongside VGO as the crude oil feedstock. They were conducted under fixed conditions: 400 °C temperature, 80 bar of $H_2$, and 5 h reaction time. It is important to note that reference catalytic and thermal experiments were also conducted without lignin to compare product yields under identical operating conditions. The absence of char formation from VGO from these experiments indicates that any char produced originates solely from lignin. For each experiment, the product yields, hydrogen consumption, conversion of hydrolysis lignin, and mass balances were calculated. This analysis enabled evaluation of product yields, monomer fractions and the catalyst's cracking activity over time. On average, the mass balance closure for all experiments, excluding hydrogen consumption, was about 95.0 % with a standard deviation of 2.3 %. The product distributions from the single-cycle hydrotreating of dry lignin in VGO obtained at different catalyst loadings are reported in Fig. 7a. Under the single-cycle hydroprocessing (HL5g–400–80–5–$W_x$, where x = 0, 5 and 20 wt%), the lignin-oil yield was higher with NiMoP ($HEP_{12}$, 79.1 wt%) compared to that without NiMoP ($HEP_{10}$, 69.8 wt%). Fig. 6a also shows that the thermal hydrotreatment ($HEP_{10}$, blank) of hydrolysis lignin resulted in a 22.8 wt% solid char yield, which was significantly suppressed to 6.5 wt% with 20 wt% catalyst loading ($HEP_{12}$). These results also indicated a high hydrogen consumption from 7.3 to 23.7 mmol/g, respectively. Comparing closely between 5 and 20 wt% NiMoP catalyst loadings ($HEP_{11}$ and $HEP_{12}$), only a small increase in lignin-oil yield was observed, but there was a pronounced water formation and hydrogen consumption with the higher catalyst loading of 20 wt%. This suggests that the catalyst in VGO promotes further depolymerization and deoxygenation reactions to produce low-boiling point products while inhibiting condensation reactions that lead to char formation.

In single-stage hydroprocessing, hydrogen consumption was 7.3 mmol/g lignin for the blank (HEP10) and 19.0 mmol/g lignin for the 5 % catalyst (HEP11), with corresponding bio-oil yields of 69.8 % and 77.5 %. The hydrogen utilization efficiency was calculated as 9.6 %/mmol $H_2$ and 4.1 %/mmol $H_2$, respectively. The 20 % catalyst loading (HEP12) showed a hydrogen consumption of 23.7 mmol/g lignin and a bio-oil yield of 79.1 %, yielding a lower hydrogen utilization efficiency of 3.3 %/mmol $H_2$. In multicycle hydroprocessing, hydrogen consumption increased further (16.87 mmol/g lignin for the blank (HEP15) and 29.3 mmol/g lignin for the 20 % catalyst (HEP17)), but the bio-oil yield also improved, with a corresponding decrease in hydrogen utilization

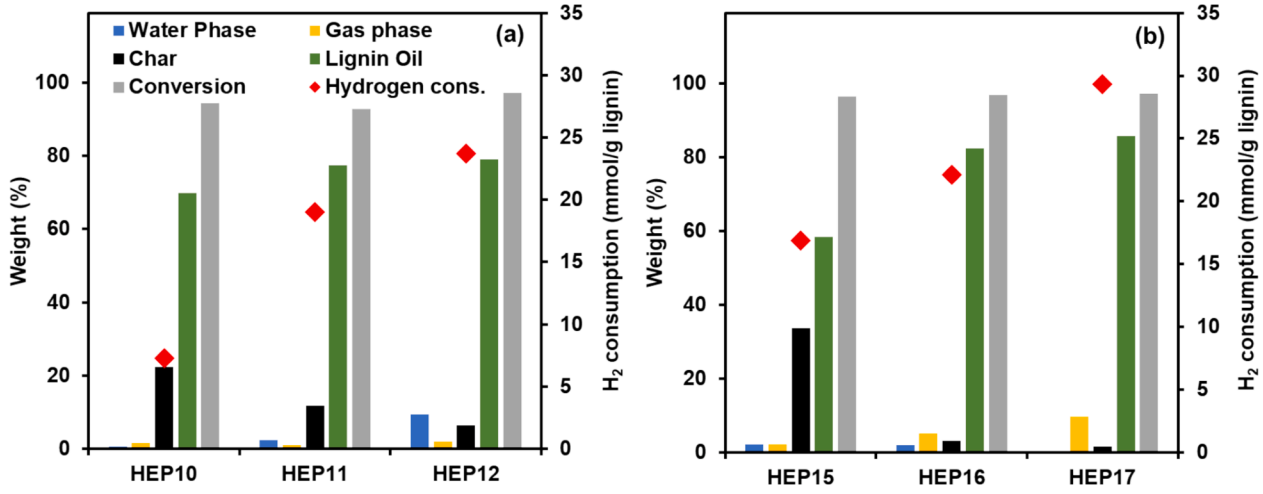


**Fig. 7.** Product distributions for thermal and catalytic conversion of hydrolysis lignin in single cycle (a) and co-multi-hydroprocessing (b) of lignin-oil blends as a function of catalyst loadings 0, 5 and 20 wt% NiMoP.

efficiency from 3.5 %/mmol $H_2$ (blank) to 2.9 %/mmol $H_2$ (20 % catalyst). As the catalyst loading increases, the hydrogen consumption also increases, which may impact the scalability of the process, as higher hydrogen consumption implies higher operating costs. However, the increased bio-oil yield with higher catalyst loadings is an important consideration for scaling up the process. From an economic perspective, it is crucial to minimize hydrogen consumption while maximizing bio-oil yield. Higher catalyst loadings lead to better bio-oil yields but at the cost of increased hydrogen consumption, which could raise operational costs. Recycle streams, such as those used in multicycle hydroprocessing, may help mitigate hydrogen consumption, offering a potential strategy for more cost-effective operation at larger scale. The multicycle hydroprocessing results suggest that repeated use of the catalyst leads to higher bio-oil yields and better hydrogen utilization, which could make this approach more economically attractive over time. The improvement in hydrogen efficiency with repeated cycles may help reduce the overall hydrogen cost, contributing to the long-term cost-effectiveness of the process. In conclusion, while hydrogen utilization efficiency decreases with higher catalyst loadings, the corresponding increase in bio-oil yield presents a trade-off that must be carefully optimized for both scalability and economic feasibility.

The key aspect of co-hydroprocessing with VGO is also the ability to convert high boiling point components (oxygenate-free compounds, b. p. > 343 °C) into lighter distillates through multicycle hydrocracking and hydrodeoxygenation of lignin-oil blends. Fig. 7b illustrates the product distribution results, demonstrating how the multicycling without catalyst led to a decline in lignin-oil yield ($HEP_{15}$: 58.3 wt%) despite a two-fold increase in hydrogen consumption. Moreover, multicycling co-hydroprocessing in absence of catalyst resulted in a higher char yield of 33.7 wt% compared to the single-cycle process ($HEP_{10}$, 22.4 wt%) which yielded more lignin-oil (69.8 wt%, Fig. 7a). This indicates the importance of including catalysts in the co-processing [56,57]. The experiments with VGO consistently demonstrated better hydroprocessing performance for both single and multicycle co-hydroprocessing (Fig. 7) compared to those with hexadecane, resulting in higher lignin-oil and lower char yields (Figs. 4 and 6a). However, the gas yields produced at 400°C and 80 bar of $H_2$ were slightly higher ($HEP_{12}$: 2.1 wt% and $HEP_{17}$: 9.6) compared to those with hexadecane ($HEP_5$: 1.5 wt% and $HEP_9$: 6.9). Furthermore, beyond 400°C, the gas yield with VGO may increase further with time and temperature, as indicated by Bergvall et. *al* [58]. Thus, the catalytic hydroprocessing of lignin with VGO or hexadecane as a solvent could strongly influence the distillate yield and the product selectivity due to differences in the composition of the co-processing feeds. The efficacy of a catalyst is intricately tied to solvent properties, encompassing polarity, proticity, and basicity [59]. Thus, a comprehensive investigation into how solvent characteristics impact reactions stands as a pivotal avenue for future research.

The elemental analysis of the lignin-oil blends is indeed crucial for evaluating the potential for deoxygenation during hydroprocessing, as plotted in Van Krevelen diagrams (Fig. 8). It is important to note that the solid residues also contain various levels of oxygenates which are not included in the oxygen mass balance. Comparing with the hydrolysis lignin feed (O/C:0.47), a substantial decline in the oxygen content (O/C: 0.019–0.15) and an increase in carbon and hydrogen contents were observed for all co-processed lignin-oil blends. Interestingly, the decrease in oxygen content is more pronounced when lignin-oil blends resulting from VGO are utilized as co-processing solvent compared to hexadecane ($HEP_9$: O/C: 0.06 vs $HEP_{17}$: O/C: 0.03), potentially indicating a stronger correlation with higher hydrogen consumption during the process (e.g., $HEP_9$: 21.5 vs $HEP_{17}$: 29.3 mmol/g). Comparing the product yields from various blends may provide confirmation of the synergistic effect in catalytic co-processing with lignin-oil blends

**Table 7**
Monomer yields and boiling-point distribution for the lignin-oils blends for co-processing with VGO as a function of catalyst loadings 0, 5 and 20 wt% NiMoP.

| Properties | $HEP_{10}$ | $HEP_{11}$ | $HEP_{12}$ | $HEP_{15}$ | $HEP_{16}$ | $HEP_{17}$ |
|---|---|---|---|---|---|---|
| *monomer distribution (GCxGC)* | *single-cycle* | | | *multicycle* | | |
| total | 49.6 | 64.1 | 71.0 | 52.9 | 71.5 | 83.4 |
| light alkanes/alkenes (< C10) | 4.3 | 6.8 | 7.5 | 2.7 | 7.7 | 10.1 |
| heavy alkanes/alkenes (>C10) | 6.1 | 7.9 | 11.6 | 10.9 | 11.6 | 12.5 |
| cycloalkanes | 1.3 | 6.5 | 9.1 | 2.0 | 5.1 | 6.7 |
| aromatics | 0.9 | 10.2 | 19.3 | 9.1 | 17.0 | 29.0 |
| ketones/alcohols | 16.5 | 18.4 | 12.3 | 10.2 | 13.2 | 16.0 |
| alkylated phenolics | 20.5 | 14.2 | 11.2 | 17.1 | 16.9 | 9.1 |
| *Sim-Dis TGA* | | | | | | |
| naphtha range (wt.%, IBP-177 °C) | 1.2 | 2.5 | 3.5 | 2.5 | 4.3 | 7.5 |
| distillate range (wt.%, 177–343 °C) | 36.0 | 49.5 | 60.5 | 65.5 | 74.7 | 84.5 |
| heavy oil range (wt.%, 343–524 °C) | 62.8 | 48.0 | 36.0 | 32 | 21.0 | 8.0 |
| residue (wt.%, > 524 °C) | 0 | 0 | 0 | 0 | 0 | 0 |

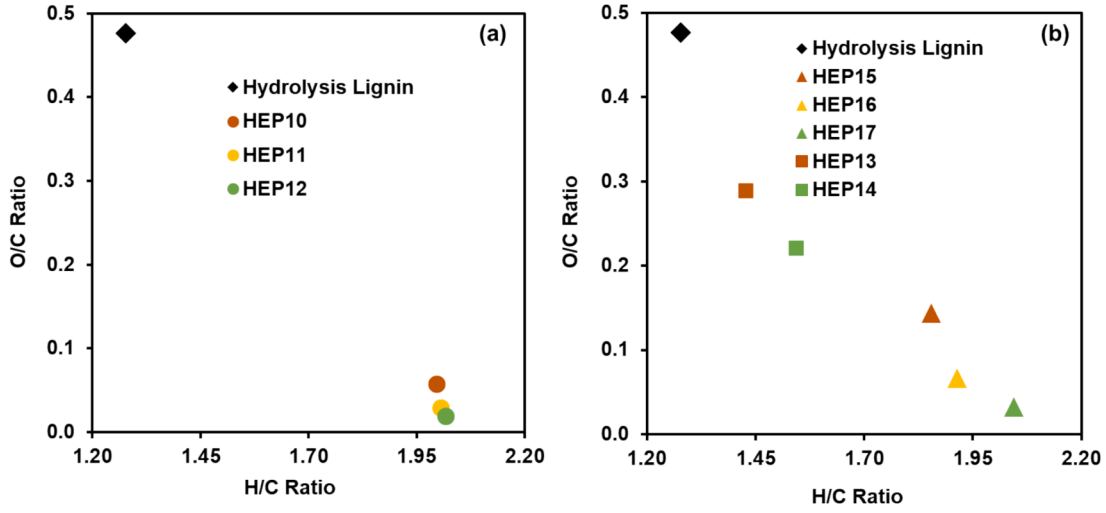


**Fig. 8.** Van Krevelen diagram for thermal and catalytic conversion of hydrolysis lignin in single cycle (a) and co-multi-hydroprocessing (b) of lignin-oil blends as a function of catalyst loadings 0, 5 and 20 wt% NiMoP. Not multicycle for HEP13 and HEP14, see Table 2.

resulting from VGO-lignin co-hydroprocessing [60]. In experiments without NiMoP catalyst, the O/C ratios for the multicycle co-hydroprocessing ($HEP_{10}$ and $HEP_{15}$) are much higher compared to the single hydroprocessing ($HEP_0$ and $HEP_7$) despite their high hydrogen consumption. Nevertheless, these results corroborate the finding when using a higher lignin loading in a single cycle hydroprocessing ($HEP_{13}$: HL10g–400–80–15–$W_0$), showing an upward in O/C and H/C ratio and a downward trend in H/C ratio (Fig. 8b). With NiMoP ($HEP_{11\text{-}12}$ and $HEP_{16\text{-}17}$), the lignin-oil blends resulted in higher H/C and lower O/C ratios along with lower char yields. These results indicate an increase in deoxygenation, particularly in experiments with higher spent catalytic loading, leading to an attenuation in repolymerization reactions and char formation during the co-multi-hydroprocessing ($HEP_{17}$: deoxygenation of 93.9 %).

The determination of boiling-point of lignin-oil blends and vacuum residues was carried out by SimDist TGA. Table 7 illustrates that the major components of the obtained lignin-oil blends fell within the temperature range of 177°C to 524°C. Less than 4 and 8 wt% were in the naphtha fraction (< 177 °C) for lignin-oil blends for the single-cycle (Table 7) and multicycle processes (Table 7), respectively. It is evident that higher NiMoP catalytic loadings tended to increase the naphtha and distillate fractions (IBP – 343 °C). Meanwhile, the proportions of other components in the heavy oil boiling range (> 343 °C) decreased with catalyst loading. Specifically, when 20 wt% NiMoP was used for the multicycle co-processing with VGO, the content of naphtha and distillate fractions reached 7.5 wt% and 84.6 wt%, respectively ($HEP_{17}$). These changes were similar for the single cycle experiments, but less pronounced. In experiments without catalyst ($HEP_{10}$ and $HEP_{15}$), the much lower paraffinic content in the naphtha fraction indicated more char formation, as observed in Fig. 7 and Table 7. These results suggest that less dealkylation reactions with no catalyst may favor recondensation reactions [61]. To further explore the SimDist TGA fractions (Table 7), the lignin-oil blends were analyzed using GCxGC/FID-MS, in which the major monomeric detectable products would be in the naphtha (< 177°C) and distillate (177 – 343°C) fractions. Table 7 reports quantities of selected hydrocarbon-types from the hydroprocessed lignin-oil blends generated at 400 °C, 80 bar of $H_2$, and co-hydroprocessed with lignin. Under these operating conditions, the lowest monomeric yields were observed for the blank experiments ($HEP_{10}$ and $HEP_{15}$). This is likely due to the prominence of recondensation reactions forming char at the given conditions when hydrolysis lignin was processed without the NiMoP catalyst (Fig. 6a and b). Particularly for the single cycle hydroprocessing, the aromatics yield was the lowest at 0.9 wt% ($HEP_{10}$). This is reasonable since aromatics and naphthenes might further recondense due to their higher reactivity (C–C formation) to form char/coke to a high extent without the catalyst [61]. It is also noticed that the naphtha fractions from the blank experiments were low at 1.2 wt% and 2.5 wt% for $HEP_{10}$ and $HEP_{15}$, respectively (Table 7). Interestingly, the high char content of $HEP_{15}$ is consistent with its lower paraffinic content of 2.7 wt %, corresponding to the naphtha fraction (light naphtha < C10: IBP to 100°C).

The aromatic and paraffin monomeric yields including cycloalkanes were enhanced for the catalytic experiments. The increased content of light naphtha and aromatic fraction yields for the multicycle co-hydroprocessing of lignin-oil blends ($HEP_{16}$ and $HEP_{17}$) suggests that dealkylation and deoxygenation reactions are promoted with higher loading of the NiMoP catalyst, corresponding with a decrease in yields of alkylated phenolics in the lignin-oil blends. It is also suggested that the lignin-oil from hydrolysis lignin contained higher yields of small alcohol and ketone molecules, which may be obtained from ring-opening of cellulose residues in the hydrolysis lignin [37]. The phenolic hydroxyl groups, also presented in Table 7, are in greater quantities in the products from the blank experiments, which are one of precursors to form condensed lignin product from the different fragments. Importantly, these phenolics in the lignin-oil blends tend to decline with NiMoP loading, giving rise to small oxygenated compounds and aromatic-naphthene compounds. The lignin-oil blends, from VGO in both single-cycle hydroprocessing ($HEP_{12}$) and multicycle co-hydroprocessing ($HEP_{17}$) experiments with 20 wt% NiMoP loading, highly promoted deoxygenation of phenolics from the lignin, resulting in high aromatic yields of 19.3 wt% and 29.0 wt%, respectively. In comparison, the lignin-oil blends from single and multicycle co-hydroprocessing with hexadecane ($HEP_5$ and $HEP_9$), gave lower aromatic yields of 16.0 wt% and 9.5 wt%, respectively. These results support the suggestion made previously that the solvents (VGO and hexadecane) and processing mode (single hydroprocessing versus co-multi-hydroprocessing cycle) have a strong effect on distillate yield, which may influence the reactivity of the lignin-oil blends.

The NiMoP catalyst in this study demonstrated high bio-oil yields of up to 93.2 % (with hexadecane) and 85.6 % (with VGO), matching or exceeding the yields obtained from other state-of-the-art catalysts [62–65]. Notably, its robustness was evident across multiple operational cycles, highlighting its longevity and efficiency for long-term hydroprocessing. In terms of product selectivity, the NiMoP catalyst showed excellent control over the distribution of bio-oil components, producing predominantly valuable aromatic hydrocarbons, which are the desired products from lignin upgrading. This high selectivity is particularly important in tailoring the catalytic process to produce specific chemicals [65–67], which can improve the economic feasibility of the process. The use of unsupported NiMoP catalysts offers significant technical advantages, particularly by eliminating the dependency on supports. This simplification avoids potential issues such as support sintering or deactivation during hydroprocessing. Additionally, the avoidance of sulfiding steps simplifies catalyst handling and extends catalyst life, reducing maintenance and operational costs. These factors contribute to the overall economic viability of the process for large-scale lignin hydroprocessing. The superior hydrogenation activity and stability of NiMoP make it a promising candidate for scalable lignin upgrading processes. Its high surface area and reduced sensitivity to sulfur contamination make it more suitable for continuous, long-term operations compared to traditional supported Mo and Ni-based catalysts.

### 3.5. *Blending optimization of hydrolysis lignin*

Considering the blending ratio of hydrolysis lignin and VGO is of importance to prevent deactivation of the catalyst during the (co–) hydroprocessing. A recent report demonstrated that a blend of liquefied biocrude with VGO ratio exceeding 10 wt% at a lower temperature of 370°C led to significant catalyst deactivation [68]. In our current study, the hydrotreating experiments involved physical mixing of dry hydrolysis lignin in VGO/hexadecane with a lignin weight fraction of 7.5 wt%. Fig. 9 compares the blending effect of catalyst-free co-hydroprocessing in hexadecane or VGO. It was clearly observed that the lignin-oil blends were fully miscible when hydrotreated with VGO and they were easily transferred from the reactor ($HEP_{10}$). However, this was not the case when co-hydroprocessing with hexadecane without catalyst ($HEP_0$). This is consistent with the multicycle co-hydroprocessing products showing a higher lignin-oil yield and lower char yield with VGO ($HEP_{15}$) compared to hexadecane ($HEP_7$). This difference may be attributed to the formation of heavier condensed oligomeric compounds while using hexadecane, which strongly adhered to the reactor vessel walls, as also shown by Cheah *et al.* [31]. This could also be explained by the formation of a lower amount of total char, with or without catalyst, present in the reactor. For instance, the set of multicycle co-hydroprocessing involving the addition of 2.5 g dry lignin ($HEP_{16\text{-}17}$, Fig. 7b) showed overall better performance for lignin-oil VGO blends, with the total formed char, including catalyst, below 10 wt%. Remarkably, it is clearly evident for the multicycling co-hydroprocessing involving hexadecane with 20 wt% NiMoP resulted in less than 10 wt% char ($HEP_9$, Fig. 6a). However, higher than 10 wt% of char was observed under identical conditions with 5 wt% NiMoP ($HEP_8$, Fig. 6a), resulting in a poor lignin-oil yield. These results underscore the importance of the blending ratio

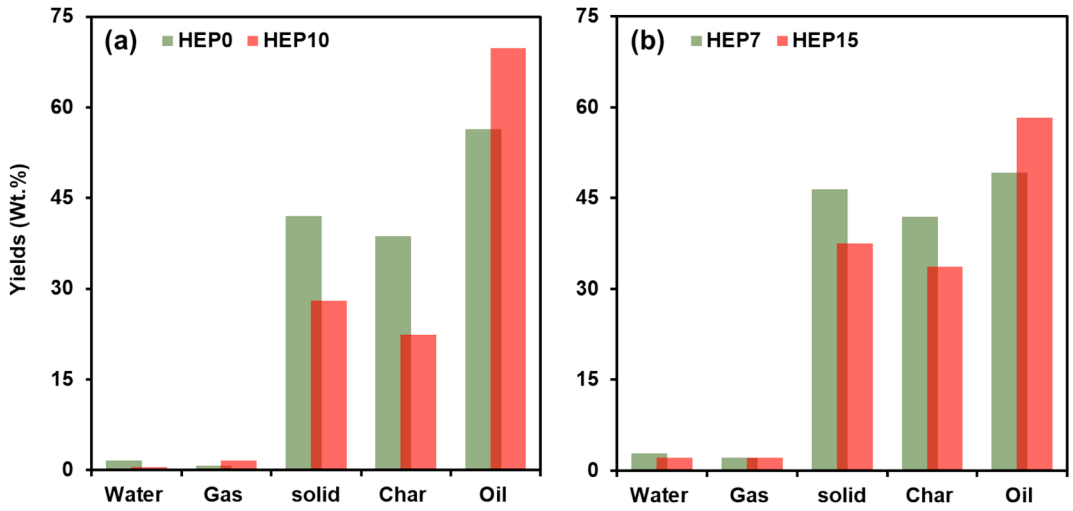


**Fig. 9.** Direct blending effect (a) for single-cycle hydroprocessing and (b) multicycle co-hydroprocessing of lignin without catalyst. Green: in hexadecane; Red: in VGO. Operating conditions: 400 °C, 80 bar of $H_2$. Reaction time: $HEP_0$ and $HEP_{10}$ for 5 h and $HEP_7$ and $HEP_{15}$ for three cycles of 5 h each. See Table 1. (For interpretation of the references to colour in this figure legend, the reader is referred to the web version of this article.)

of lignin and solvent-type synergy for higher catalytic performance in a recirculated system to achieve low-cost production of bio-fuel. In the following section, the feasibility and comparison of lignin hydroprocessing along with VGO at a higher initial lignin amount (10 g) is investigated.

In multicycle hydroprocessing experiments, the accumulation of spent catalyst and unconverted lignin significantly influences subsequent reaction cycles, particularly in terms of char formation, product distribution, and overall process efficiency. Our results highlight that higher catalyst loadings effectively suppress char formation and reduce unconverted lignin, thereby enhancing process performance. For hydroprocessing with hexadecane, the uncatalyzed reaction (HEP7) resulted in a char yield of 42 % and 4.5 % unconverted lignin. Introducing a 5 % catalyst loading (HEP8) reduced the char yield to 16.9 %, although unconverted lignin increased marginally to 5.5 %. At a higher catalyst loading of 20 % (HEP9), char formation was further minimized to 5.0 %, with unconverted lignin significantly decreasing to 1.9 %. A similar trend was observed for hydroprocessing with VGO. The uncatalyzed reaction (HEP15) yielded 33.7 % char and 3.7 % unconverted lignin. The addition of 5 % catalyst (HEP16) substantially reduced the char yield to 3.1 %, with a slight reduction in unconverted lignin to 3.2 %. Increasing the catalyst loading to 20 % (HEP17) further reduced char formation to 1.6 %, while unconverted lignin decreased to 2.9 %. These results accentuate the significant role of catalyst loading in enhancing deoxygenation and dealkylation reactions, which are critical for char suppression and the efficient conversion of lignin into valuable bio-oil products.

The correlation between catalyst loading and char suppression is particularly evident when comparing the hexadecane and VGO systems. VGO demonstrated a more pronounced reduction in char formation and unconverted lignin, likely due to its superior compatibility with the catalytic system and its ability to promote reactions that favor the formation of naphthenes and aromatics. This enhanced reactivity emphasizes the importance of catalyst versus lignin-oil formed interactions in multicycle hydroprocessing. Although the NiMoP catalyst exhibited robust performance across multiple cycles, the accumulation of residues and catalyst fouling could alter product distribution and catalyst activity during extended operations. Strategies such as periodic catalyst regeneration (e.g., mild oxidation or hydrogen treatment) and removal of unconverted lignin residues may be necessary to maintain catalyst activity and reaction efficiency in long-term processes. The observed trends in this study highlight the potential for optimizing catalyst loading and lignin-oil solvent selection to mitigate residue accumulation, minimize char formation, and sustain high yields of valuable products in multicycle hydroprocessing.

### 3.6. *Case study for higher lignin blend ratio hydroprocessing*

Processing of dry lignin has been proven to be extremely challenging within the existing refinery infrastructure. In order to better comprehend a potential processing method and the reactivity of lignin in VGO or lignin-oil blends, we investigated the feasibility of processing hydrolysis lignin at a higher feed ratio alongside VGO. Two sets of experiments were conducted under identical conditions. Initially, a lignin-VGO blend was hydroprocessed at a high starting feed of 10 g of lignin, for 15 h ($HEP_{13}$ and $HEP_{14}$, as detailed in Table 2, constituting a single-cycle experiment, for the case without and with catalyst). Experiments $HEP_{13}$ and $HEP_{14}$ were also intermittently halted every 5 h without the addition of fresh lignin, to facilitate a comparison against the multicycle experiments $HEP_{15}$ and $HEP_{17}$. Following the collection and evacuation of the gaseous product, fresh hydrogen gas was introduced into the reactor in order to continue the hydroprocessing. After a total reaction time of 15 h, the resulting products were characterized using the aforementioned methods and subsequently compared to the results obtained from $HEP_{15}$ and $HEP_{17}$ (Table 2 and Fig. 1b), wherein the same 10 g of lignin was intermittently fed during the same 15 h of reaction time, i.e. a multi-cycle experiment. The objective was to understand the effect of multicycling and establish an operating window that favors an acceptable lignin-VGO blend ratio for implementation.

Fig. 10 illustrates the impact of the two processing schemes with varying initial lignin feed on hydrodeoxygenation activity over blank and catalyzed experiments. It is immediately apparent that the product distributions are affected by the high feed ratio (10 g of lignin in VGO: $HEP_{13}$ and $HEP_{14}$) compared to intermittent feeding (5 g lignin in VGO initially, then 2.5 g and finally 2.5 g: $HEP_{15}$ and $HEP_{17}$). For the blank experiments, the lignin-oil yield decreased while increasing the char and gas yields when a high lignin-VGO blend was supplied ($HEP_{13}$, Fig. 10a). Whereas with the multicycle experiments ($HEP_{15}$), lower gas and higher lignin oil yields were observed compared to the case with 10 g lignin-VGO initial blend. The result suggests that adding small portions of lignin in multicycling experiments inhibits char formation. It is possible that the molecules formed from the hydrolysis lignin, such as aldehydes and ketones, result in less char formation when lignin is added in the second and third cycle. In our previous study, we suggested that the lower char amount when using hydrolysis lignin compared to kraft lignin was due to reactions with small molecules formed from the

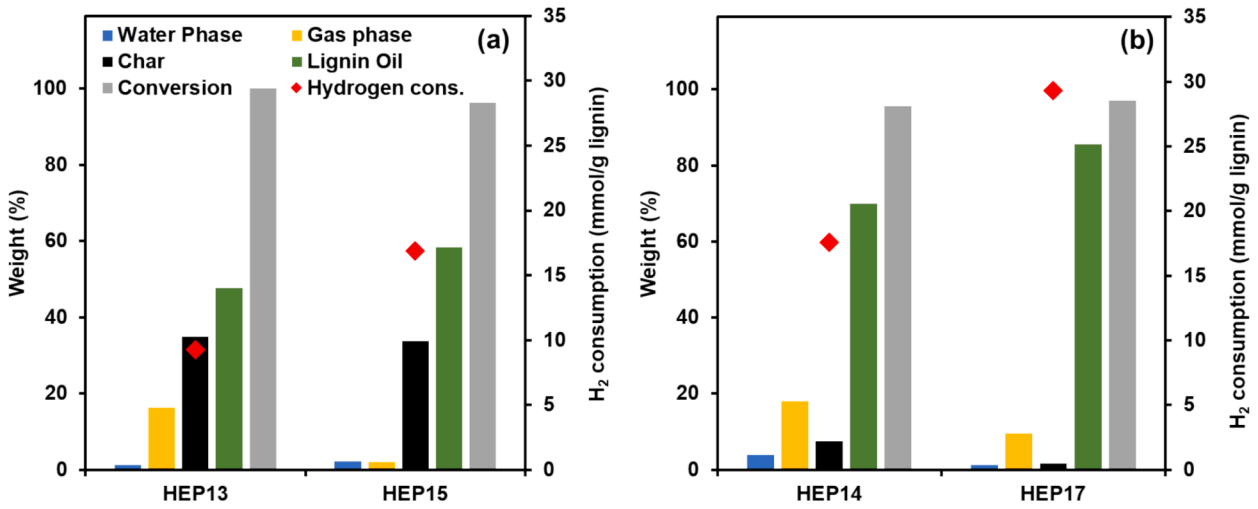


**Fig. 10.** Product distributions and hydrogen consumption of (a) thermal and (b) catalytic experiments. Operating conditions: 400 °C, 80 bar. $HEP_{13}$ and $HEP_{14}$ are single cycle experiments using 10 g of lignin for 15 h, without and with catalyst respectively. $HEP_{15}$ and $HEP_{17}$ are multi cycle experiments using 5 + 2.5 + 2.5 g of lignin for 5 + 5 + 5 h, without and with catalyst, respectively.

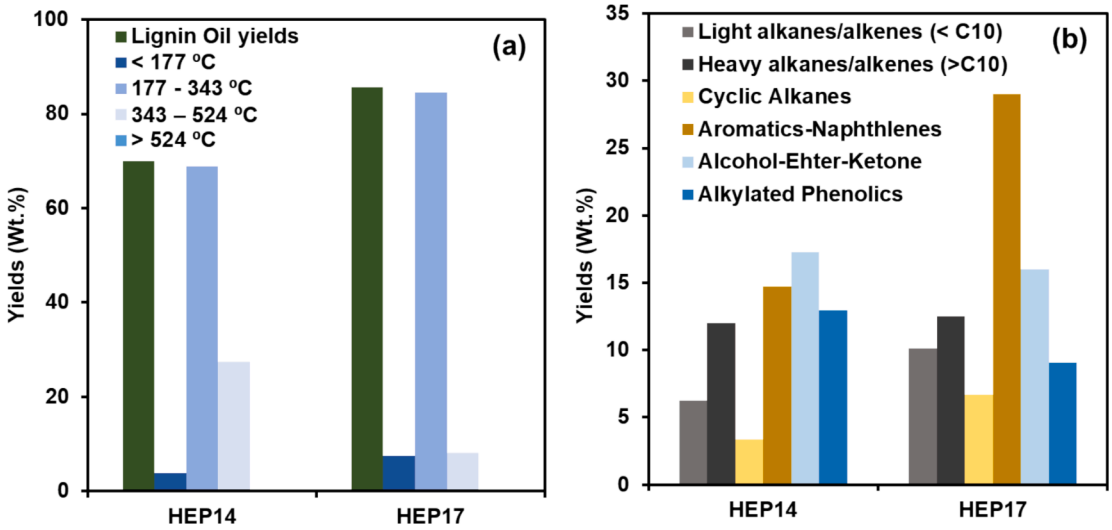


**Fig. 11.** (a) SimDist distributions and (b) monomer yields by GCxGC analysis. Operating conditions: 400 °C, 80 bar. $HEP_{14}$ is single cycle experiments using 10 g of lignin for 15 h, with catalyst. $HEP_{17}$ is multi cycle experiments using 5 + 2.5 + 2.5 g of lignin for 5 + 5 + 5 h, with catalyst.

hydrolysis lignin [37]. These results are similar to those of the catalytic experiments. A substantial decrease in lignin-oil was observed for the 10 g lignin-VGO initial blend ($HEP_{14}$: 70.0 wt% vs. $HEP_{17}$: 85.6 wt%, Fig. 10b) and simultaneously a higher char and gas yields of 7.4 and 18.0 wt%, respectively. Thus, also when using catalyst, co-multicycling hydroprocessing gave higher bio-oil yield as well as lower char amount. Moreover, the multicycling resulted in a higher quality of the bio-oil with lower O/C ratio ($HEP_{14}$ with O/C: 0.22 vs. $HEP_{17}$ with O/C: 0.03).

Furthermore, the boiling-point distributions of the obtained lignin-oil blends were explored as shown in Fig. 11a. Overall, differences in the product boiling-point distribution were observed when lignin was fed intermittently. It is evident that intermittent lignin feed increased the naphtha and distillate fractions (IBP-343 °C) at the expense of the heavy gas oils (343–524 °C), which reduced from 27.4 wt% to 8 wt% (Fig. 10a). Thus, the multicycle hydroprocessing of dry lignin to the lignin-oil/VGO blend improves the efficiency of conversion to lignin-oil and the distillate fraction product range. A more pronounced deactivation of catalyst active sites may be caused by the high lignin-VGO feed ratio that is likely to generate harmful reaction products as reported by Chen et. al. [69] for co-processing HTL biocrude in VGO. Therefore, an additional consideration would be to investigate more regarding the poisoning effect of the high lignin-VGO feed ratio. Paraffins, naphthene-aromatic and oxygenated compounds are identified by GCxGC/MS for a high feed ratio of lignin-VGO blend ($HEP_{14}$). Fig. 11b shows that the yield of aromatics products is strongly favored by intermittent multi-cycle co-hydroprocessing ($HEP_{17}$) compared to non-intermittent co-hydroprocessing ($HEP_{14}$). Also, it can be observed that yield of oxygenated compounds is higher for $HEP_{14}$, which enhances the content of phenolic hydroxyl groups and may produce condensed lignin products from the different fragments. This may be attributed to differences in the reactivity of the lignin-oil blends, and thus further affect the distillate fractions.

### 3.7. Funnel plot assessment

Through the aforementioned experiments, both single cycle and multicycle hydroprocessing alongside petroleum intermediates have been investigated for direct integration of hydrolysis lignin into existing petrorefinery processes. Interestingly, multicycle co-hydroprocessing exhibited superior performance in terms of energy recovery,

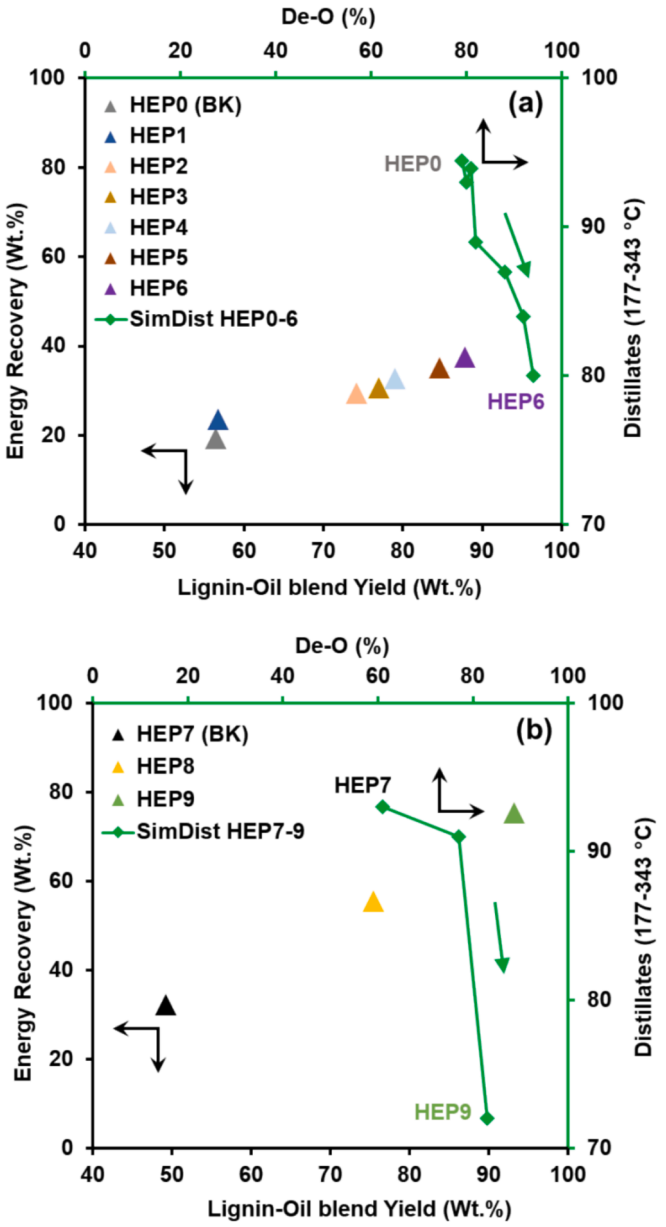


**Fig. 12.** Funnel plot representing energy recovery vs lignin-oil blend yields, and deoxygenation degree vs. distillate yields for single cycle (a) and multicycle (b) co-hydroprocessing of lignin-oil blends with and without NiMoP catalyst in hexadecane.

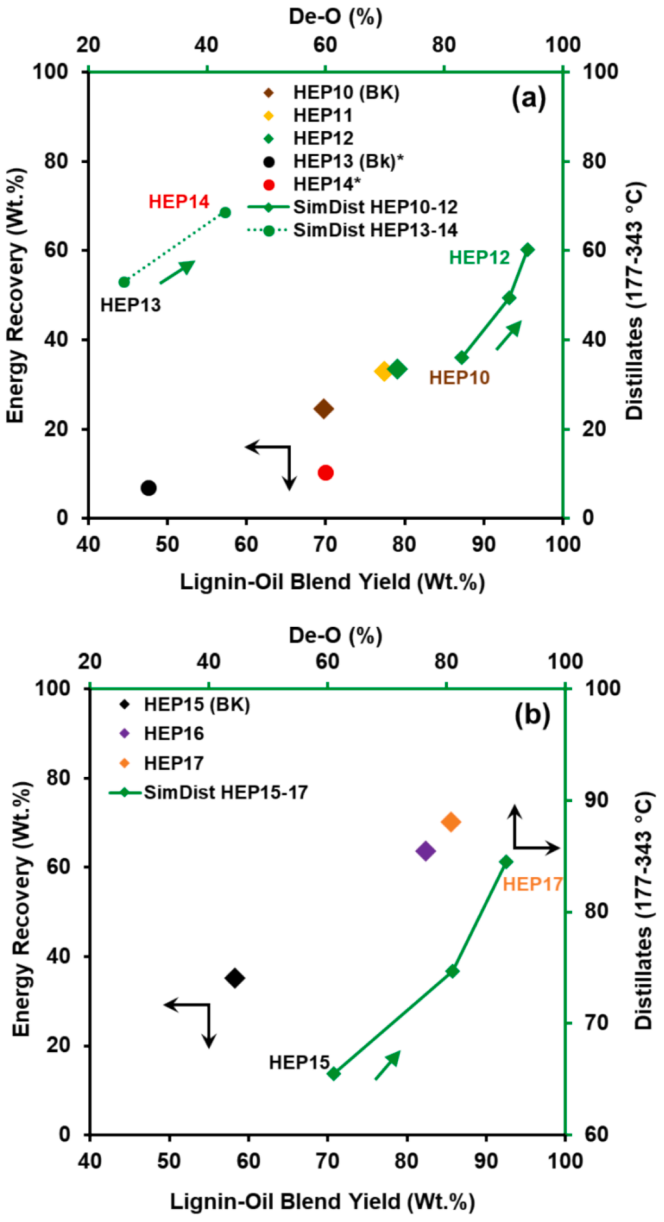


**Fig. 13.** Funnel plot representing energy vs lignin-oil blend yields, and deoxygenation degree vs. distillate yields for single cycle (a) and multicycle (b) co-hydroprocessing of lignin-oil blends with and without NiMoP catalyst in VGO.

deoxygenation degree, and lignin-oil yields, as well as a notable enhancement in distillate fractions (177–343 °C), particularly when VGO was involved. To assess the findings, a funnel plot is introduced as a graphical method to analyze and compare the experimental performance. It is important to note that the funnel plot is solely utilized to assess the quality of similar processes. Figs. 12 and 13 depict a funnel plot of processes transforming hydrolysis lignin to finished fuel via single and multicycle hydroprocessing in like-heavy straight run naphtha (HSR) and VGO. The energy yield was calculated from overall lignin-oil based on dry and ash-free conditions, and the energy density of the products was calculated using the Higher Heating Value (HHV) of the lignin-oil obtained after each reaction. The energy and lignin-oil blend yields are located at the bottom left of the funnel. The deoxygenation degree and distillate yields are included at the top right. These axes not only aid in plotting data but also effectively highlight the practical limitations for converting hydrolysis lignin into transportation fuels.

Fig. 12 represents single and multicycle co-hydroprocessing in hexadecane, respectively. For single-cycle lignin hydrotreating in hexadecane, the lignin-oil yield increased with temperature, pressure, and catalyst loading (Fig. 12a, top), accompanied by an enhancement in energy yield. Conversely, the distillate fraction (177–343 °C) showed an opposite trend despite the improvement in deoxygenation and thus energy recovery. Yield losses in the distillate fraction appeared as an increase in the naphtha fraction, which rose from 3.6 to 17.6 wt% (Table 5, $HEP_0$ to $HEP_6$), accompanied with higher De-O and lower char formation.

NiMoP had a more pronounced impact on isomeric hydrocarbons rather than aromatics. This suggests that in reactions with NiMoP, cellulose units in hydrolysis lignin undergo partial hydrodeoxygenation to form oxygenated compounds and subsequently hydrocarbons. This aligns with results from catalytic hydrogenation of cellulose to hydrocarbons using hexadecane as a solvent [45]. Previous studies using

model compounds over NiMo/MoP/$Ni_2P$ [39,40] support this, indicating that the active sites of Ni2P catalysts, composed of threefold hollow Ni and P sites, facilitate adsorption of H or OH groups. Further aromatization was slightly enhanced ($HEP_7$ to $HEP_9$), as phenolic yields decreased, indicating that co-processing over NiMoP using hexadecane enhances hydrocracking activity rather than alkylation reactions. This was also confirmed for $Ni_2P$/HZSM-5 catalysts, attributed to strong acid sites promoting hydrocracking and isomerization reactions [48]. Another hypothesis is that the quantity of water significantly affects the maximum C < 10 alkane yield (see HEP8, Fig. 10b), depending on the solvent choice, as demonstrated by Deneyer et *al.* for cellulose-to-alkane conversion in a fossil naphtha/water system over a Ru on carbon catalyst. These findings suggest that lignin-oil solubility and miscibility in hexadecane significantly influences the lignin's cohesive energy density during the reaction.

A similar trend was observed for the multicycle co-hydroprocessing of lignin-oil blends with lignin (Fig. 12b). Despite the high energy and lignin-oil yields, further distillate range losses were associated with higher naphtha range (IBP-177 °C) yields, increasing from 5.5 wt% ($HEP_7$) to 41.0 wt% ($HEP_9$). This increase was marked by the rise in quantities of heavy alkanes/alkenes (> C10), cycloalkanes, and oxygenates, as demonstrated by GCxGC analysis. The production of higher alkanes/alkenes (> C10) might also result from the hydrocracking of hexadecane and aromatic-naphthalenes, the hydrotreatment of cellulosic units present in hydrolysis lignin and depolymerization of phenolic dimers [70]. The latter components were subsequently reduced to low alkylated phenolics and higher aromatics, as a function of temperature, pressure, and catalyst loading (Tables 5 and 6). Notably, yields of gaseous compounds were not excessive, particularly during multicycling. Further studies on co-hydroprocessing of model lignin components alongside hexadecane over unsupported NiMoP are of importance to understand the solubility of lignin. This could help determine whether using petroleum paraffin as the primary solvent or co-solvent is feasible for drop-in bio-fuels (Fig. 11a), as indicated by the secondary y-axis in the plot (Fig. 11b).

Fig. 13 shows funnel plots of single and multicycle co-hydroprocessing in VGO, respectively. When VGO was used for co-hydroprocessing, the energy and lignin-oil yields were slightly lower compared to paraffinic petroleum co-processing for both single cycle and multicycle processes. However, there was a clear enhancement in the quality of the lignin-oil blend from multicycle co-hydroprocessing, as evident by the increased distillate range, reaching up to 85 wt% while achieving higher energy and lignin-oil yields with the lowest oxygen contents ($HEP_{17}$). Additionally, the hypothesis of the effect of water on the C < 10 isomeric hydrocarbon production was less pronounced with VGO as a solvent compared to hexadecane and Deneyer et *al.* study for cellulose-to-alkane conversion in a light straight run naphtha (LSR) [32]. The isomeric hydrocarbons yielded were near equal parts aromatics (29.0 %) and isomeric hydrocarbons (29.3 %).

In terms of GCxGC analysis, the increase of distillate range products was apparently also influenced by the monomer distribution, particularly by the rise in aromatics (Table 7), and decreases in alkylated phenolics yields, respectively. This suggests that the catalyst in VGO promotes further depolymerization and deoxygenation reactions to produce lower-boiling point products while inhibiting condensation reaction leading to char formation. This also demonstrates the influence of the solubility of lignin in VGO, reflecting the cohesive energy density of lignin during the catalytic reaction at elevated temperature. An opposite trend was observed during the co-hydroprocessing of a higher initial amount of hydrolysis lignin (> 10 wt%) with VGO (Fig. 13a, green dashed), where twice the amount of lignin was used with and without catalyst (HEP13 and HEP14). With the NiMoP catalyst, lower aromatic (14.7 %) and higher oxygenate (30.2 %) compound yields (see Fig. 11b) were observed, confirming that VGO as a solvent has a limited capacity for blending. It was also found that the oxygen content from the lignin-oil blend during hydroprocessing with a high initial lignin feed (HEP14) also resulted in lower energy and lignin-oil yields, compared to a multicycle feed of the same total amount of lignin (HEP17). The lower yields are due to higher solids formation as well as to higher yields of permanent gases such as $CO_2$, as displayed in Fig. 10. Overall, the results suggest that a multicycle co-hydroprocessing method yields higher energy and lignin-oil yields. However, the choice of solvent, its initial boiling point range and hydrocracking, can lead to significant distillate range losses, emphasizing the importance of considering the choice of solvent in lignin conversion processes.

### 3.8. Proposed strategies for process scale up

The process of scaling up co-hydroprocessing of lignin with NiMoP catalysts requires key challenges to be addressed, such as catalyst recycling, hydrogen availability, and the integration of lignin feedstocks into existing refinery operations. Several strategies can be proposed to overcome these challenges and ensure process efficiency and economic feasibility.

First, catalyst deactivation must be minimized for efficient scaling. Periodic catalyst regeneration, such as hydrogen treatment or mild oxidation, can help maintain the NiMoP catalyst activity over extended cycles. A detailed regeneration protocol, possibly involving fluidized bed systems or batch reactors, could enhance the economic feasibility of continuous processing by reducing the need for frequent catalyst replacement. In large-scale operations, continuous catalytic regeneration could be implemented, where part of the catalyst is withdrawn, regenerated, and reintroduced to the reactor. This ensures consistent catalyst activity while minimizing costly large-scale catalyst replacement. Additionally, effective separation and recovery of spent catalyst particles from the liquid phase are crucial for maintaining a stable reaction environment. Techniques such as filtration or centrifugation can facilitate catalyst recovery and prevent its loss, while also minimizing the buildup of unconverted lignin. To improve economic feasibility and ensure continuous hydrogen supply, on-site hydrogen generation should be integrated into the process. This can be achieved through water electrolysis, ideally powered by renewable electricity, or through natural gas reforming methods like steam methane reforming. Optimizing reaction conditions, such as pressure, temperature, and hydrogen partial pressure, will be critical to minimize hydrogen consumption per unit of lignin processed. Improving the hydrogenation efficiency of the NiMoP catalyst could further reduce hydrogen demand. Additionally, recovering unreacted hydrogen from the off-gases using technologies like pressure swing adsorption (PSA) or membrane separation can allow for hydrogen recycling, reducing the overall hydrogen requirements and associated costs.

Lignin integration into refinery processes requires effective pretreatment methods to convert it into a suitable form for hydroprocessing. Pretreatment techniques such as acid or base catalysis, organosolv processes, or supercritical fluid processing can solubilize lignin, making it more amenable to hydroprocessing. Reactor design modifications, such as adapting catalyst beds to account for lignin's reactivity, or implementing advanced feedstock management techniques, will be necessary to facilitate this integration. A techno-economic analysis should be conducted to evaluate the economic feasibility of scaling up lignin hydroprocessing. This analysis should account for costs associated with lignin pretreatment, catalyst regeneration, hydrogen supply, and integration. Furthermore, it should consider the value of the products, such as biofuels and chemicals derived from lignin, market demand, and potential government incentives for renewable energy projects. As lignin hydroprocessing is energy-intensive, strategies to reduce energy consumption, such as optimizing reaction conditions and integrating energy recovery systems (e.g., heat exchangers or combined heat and power systems), will be critical for improving economic viability.

## 4. Conclusions

In this study, two scenarios were investigated for catalytic hydrotreatment of hydrolysis lignin: (1) lignin-oil blends were produced alongside hexadecane or VGO as solvents. (2) The blends, along with fresh lignin, were further co-hydroprocessed over a spent unsupported NiMoP in a multicycle scheme. The conclusions drawn from this work are as follows:

- The nanocasting synthesis of the unsupported NiMoP resulted in a catalyst with a large specific surface area, pore volume, and catalytic activity that demonstrated successful co-hydroprocessing performance.
- Hydroprocessed lignin in hexadecane exhibited a high deoxygenation activity, significantly influencing the yield of aliphatic hydrocarbons over aromatics. Under conditions of 400 °C and 80 bar pressure, the alkane-derived yield, including cycloalkanes reached as high as 41.1 wt% from the lignin-oil.
- Co-hydroprocessing of fresh lignin along with lignin-oil of hexadecane blending resulted in a significant increase in lignin-oil yield and char suppression. SimDist and GCxGC analyses demonstrated cracking activity, resulting in the production of aliphatic paraffin hydrocarbons. Higher catalyst loading favored the production of naphtha and light gas oil fractions, highlighting the efficiency of co-hydroprocessing.
- Co-processing of lignin-oil with VGO showed higher lignin-oil yield, with the lowest char yield. Product selectivity favored higher naphthene and aromatic yields, and increased content of light naphtha and aromatic fraction yields for the multicycle processing of lignin-oil blends, suggesting a promotion of dealkylation and deoxygenation reactions with higher loading of the NiMoP catalyst.
- Higher hydrogen consumption, particularly observed in the multicycling along with lignin-oil of VGO blending, correlated well with higher lignin-oil yield and lower char formation, promoting hydrogen solubility in the lignin-oil blends and thus the production of high-quality liquid fuel products.
- Solvent effects (VGO and hexadecane) and the co-processing scheme (single or multicycle) strongly influenced the distillate fraction, selectively upgrading the lignin-oil to higher quality, and affecting synergistic effects of lignin-oil blends. Interestingly, multicycling resulted in higher bio-oil yield and lower char formation compared to using the same amount of lignin in just one cycle with equal total residence times.
- Multicycle co-hydroprocessing demonstrates superior performance over single-step hydroprocessing, as qualitatively assessed via a funnel plot, for the product quality, distillate range of jet and marine drop-in fuels (177 – 343 °C) and mass and energy yields, particularly when utilizing VGO.
- The choice of solvent, especially its initial boiling point range, significantly influences the final distillate range yield of the products, due to simultaneous solvent hydrocracking. This highlights the importance of solvent selection in lignin conversion processes.

## CRediT authorship contribution statement

**Abdenour Achour:** Writing – review & editing, Writing – original draft, Methodology, Investigation, Formal analysis, Conceptualization, Supervision. **Anna Anttila:** Methodology, Investigation, Formal analysis. **Derek Creaser:** Writing – review & editing, Supervision, Conceptualization, Investigation, Methodology. **Louise Olsson:** Writing – review & editing, Supervision, Methodology, Investigation, Funding acquisition, Conceptualization.

## Declaration of competing interest

The authors declare that they have no known competing financial interests or personal relationships that could have appeared to influence the work reported in this paper.

## Acknowledgements

We would like to thank Sekab for kindly providing us the hydrolysis lignin. We would like to acknowledge Vinnova (Climate-Leading Process Industry), Swedish Energy Agency (P47511-1) and Formas (FR2021/0005) for the funding. We would like to thank Chalmers Material Characterization Laboratory (CMAL) for CHNS-O, XRD, SEM and HRTEM access/measurements.

## Data availability

Data will be made available on request.

## References

[1] Balat M. Global Status of Biomass Energy Use. Energy Sources Part A 2009;31:1160–73. https://doi.org/10.1080/15567030801952201.
[2] Rajesh Banu J, Preethi S, Kavitha VK, Tyagi M, Gunasekaran OP, Karthikeyan GK. Lignocellulosic biomass based biorefinery: A successful platform towards circular bioeconomy. Fuel 2021;302:121086. https://doi.org/10.1016/j.fuel.2021.121086.
[3] IEA, Net Zero by 2050, Paris, 2021. https://www.iea.org/reports/net-zero-by-2050.
[4] Abdulkareem FA, Padmanabhan E. Applied techniques for residual oil recovery from source rocks: A review of current challenges and possible developments. Can J Chem Eng 2023;20:4513–20. https://doi.org/10.1002/cjce.23838.
[5] Cruz PL, Montero E, Dufour J. Modelling of co-processing of HDO-oil with VGO in a FCC unit. Fuel 2017;196:362–70. https://doi.org/10.1016/j.fuel.2017.01.112.
[6] Mishra RK, Mohanty K. Characterization of non-edible lignocellulosic biomass in terms of their candidacy towards alternative renewable fuels. Biomass Convers Biorefin 2018;8:799–812. https://doi.org/10.1007/s13399-018-0332-8.
[7] M.S. Rana, V. Sámano, J. Ancheyta, J.A.I. Diaz, A review of recent advances on process technologies for upgrading of heavy oils and residua, 1894. doi: 10.1016/j.fuel.2006.08.004.
[8] H.K. Jeswani, A. Chilvers, A. Azapagic, Environmental sustainability of biofuels: a review, Proceedings of the Royal Society A: Mathematical, Physical and Engineering Sciences 476 (2020) 20200351. doi: 10.1098/rspa.2020.0351.
[9] Bellussi G, Rispoli G, Landoni A, Millini R, Molinari D, Montanari E, et al. Hydroconversion of heavy residues in slurry reactors: Developments and perspectives. J Catal 2013;308:189–200. https://doi.org/10.1016/j.jcat.2013.07.002.
[10] E. Tiffany, (12) United States Patent (10) Patent No .: Purified Syngas, 1894.
[11] Lindfors C, Elliott DC, Prins W, Oasmaa A, Lehtonen J. Co-processing of Biocrudes in Oil Refineries. Energy Fuel 2023;37:799–804. https://doi.org/10.1021/acs.energyfuels.2c04238.
[12] Bezergianni S, Dimitriadis A, Kikhtyanin O, Kubička D. Refinery co-processing of renewable feeds. Prog Energy Combust Sci 2018;68:29–64. https://doi.org/10.1016/j.pecs.2018.04.002.
[13] van Dyk S, Su J, Mcmillan JD, J.. (John) Saddler, Potential synergies of drop-in biofuel production with further co-processing at oil refineries. Biofuels Bioprod Biorefin 2019;13:760–75. https://doi.org/10.1002/bbb.1974.
[14] Al-Sabawi M, Chen J, Ng S. Fluid Catalytic Cracking of Biomass-Derived Oils and Their Blends with Petroleum Feedstocks: A Review. Energy Fuel 2012;26:5355–72. https://doi.org/10.1021/ef3006417.
[15] Fogassy G, Thegarid N, Schuurman Y, Mirodatos C. From biomass to bio-gasoline by FCC co-processing: effect of feed composition and catalyst structure on product quality. Energy Environ Sci 2011;4:5068–76. https://doi.org/10.1039/C1EE02012A.
[16] Talmadge MS, Baldwin RM, Biddy MJ, McCormick RL, Beckham GT, Ferguson GA, et al. A perspective on oxygenated species in the refinery integration of pyrolysis oil. Green Chem 2014;16:407–53. https://doi.org/10.1039/C3GC41951G.
[17] Samolada MC, Baldauf W, Vasalos IA. Production of a bio-gasoline by upgrading biomass flash pyrolysis liquids via hydrogen processing and catalytic cracking. Fuel 1998;77:1667–75. https://doi.org/10.1016/S0016-2361(98)00073-8.
[18] French R, Czernik S. Catalytic pyrolysis of biomass for biofuels production. Fuel Process Technol 2010;91:25–32. https://doi.org/10.1016/j.fuproc.2009.08.011.
[19] de Miguel Mercader F, Groeneveld MJ, Kersten SRA, Way NWJ, Schaverien CJ, Hogendoorn JA. Production of advanced biofuels: Co-processing of upgraded pyrolysis oil in standard refinery units. Appl Catal B 2010;96:57–66. https://doi.org/10.1016/j.apcatb.2010.01.033.
[20] Dada TK, Sheehan M, Murugavelh S, Antunes E. A review on catalytic pyrolysis for high-quality bio-oil production from biomass. Biomass Convers Biorefin 2023;13:2595–614. https://doi.org/10.1007/s13399-021-01391-3.
[21] Venderbosch RH. A Critical View on Catalytic Pyrolysis of Biomass. ChemSusChem 2015;8:1306–16. https://doi.org/10.1002/cssc.201500115.

[22] Lazaridis PA, Fotopoulos AP, Karakoulia SA, Triantafyllidis KS. Catalytic fast pyrolysis of kraft lignin with conventional, mesoporous and nanosized ZSM-5 zeolite for the production of alkyl-phenols and aromatics. Front Chem 2018;6. https://doi.org/10.3389/fchem.2018.00295.

[23] Custodis VBF, Karakoulia SA, Triantafyllidis KS, Van Bokhoven JA. Catalytic Fast Pyrolysis of Lignin over High-Surface-Area Mesoporous Aluminosilicates: Effect of Porosity and Acidity. ChemSusChem 2016. https://doi.org/10.1002/cssc.201600105.

[24] Vasalos IA, Lappas AA, Kopalidou EP, Kalogiannis KG. Biomass catalytic pyrolysis: process design and economic analysis, WIREs. Energy Environ 2016;5:370–83. https://doi.org/10.1002/wene.192.

[25] Agblevor FA, Mante O, McClung R, Oyama ST. Co-processing of standard gas oil and biocrude oil to hydrocarbon fuels. Biomass Bioenergy 2012;45:130–7. https://doi.org/10.1016/j.biombioe.2012.05.024.

[26] Melin K, Strüven JO, Eidam P, Appelt J, Hummel C, Armbruster U, et al. Hybrid Gasoline Production from Black Liquor through Coprocessing. Energy Fuel 2022;36:12004–9. https://doi.org/10.1021/acs.energyfuels.2c01638.

[27] Pinheiro A, Dupassieux N, Hudebine D, Geantet C. Impact of the Presence of Carbon Monoxide and Carbon Dioxide on Gas Oil Hydrotreatment: Investigation on Liquids from Biomass Cotreatment with Petroleum Cuts. Energy Fuel 2011;25:804–12. https://doi.org/10.1021/ef1012769.

[28] Han Y, Pires APP, Garcia-Perez M. Co-hydrotreatment of the Bio-oil Lignin-Rich Fraction and Vegetable Oil. Energy Fuel 2020;34:516–29. https://doi.org/10.1021/acs.energyfuels.9b03344.

[29] Alvarez-Majmutov A, Badoga S, Chen J, Monnier J, Zhang Y. Co-Processing of Deoxygenated Pyrolysis Bio-Oil with Vacuum Gas Oil through Hydrocracking. Energy Fuel 2021;35:9983–93. https://doi.org/10.1021/acs.energyfuels.1c00822.

[30] Grilc M, Veryasov G, Likozar B, Jesih A, Levec J. Hydrodeoxygenation of solvolysed lignocellulosic biomass by unsupported MoS2, MoO2, Mo2C and WS2 catalysts. Appl Catal B 2015;163:467–77. https://doi.org/10.1016/j.apcatb.2014.08.032.

[31] Cheah YW, Intakul R, Salam MA, Sebastian J, Ho PH, Arora P, et al. Slurry co-hydroprocessing of Kraft lignin and pyrolysis oil over unsupported NiMoS catalyst: A strategy for char suppression. Chem Eng J 2023;475:146056. https://doi.org/10.1016/j.cej.2023.146056.

[32] Deneyer A, Peeters E, Renders T, Van den Bosch S, Van Oeckel N, Ennaert T, et al. Direct upstream integration of biogasoline production into current light straight run naphtha petrorefinery processes. Nat Energy 2018;3:969–77. https://doi.org/10.1038/s41560-018-0245-6.

[33] Del Bianco A, Panariti N, Di Carlo S, Elmouchnino J, Fixari B, Le Perchec P. Thermocatalytic hydroconversion of heavy petroleum cuts with dispersed catalyst. Appl Catal A Gen 1993;94:1–16. https://doi.org/10.1016/0926-860X(93)80041-N.

[34] Zhang H, Lin H, Zheng Y. Deactivation study of unsupported nano MoS2 catalyst. Carbon Resour Convers 2020;3:60–6. https://doi.org/10.1016/j.crcon.2019.09.003.

[35] Iwata Y, Araki Y, Honna K, Miki Y, Sato K, Shimada H. Hydrogenation active sites of unsupported molybdenum sulfide catalysts for hydroprocessing heavy oils. Catal Today 2001;65:335–41. https://doi.org/10.1016/S0920-5861(00)00554-X.

[36] Wang J, Fu Y, Chen H, Shen J. Effect of supports on the supported Ni2P catalysts prepared by the phosphidation using triphenylphosphine in liquid phase. Chem Eng J 2015;275:89–101. https://doi.org/10.1016/j.cej.2015.03.129.

[37] Achour A, Bernin D, Creaser D, Olsson L. Evaluation of kraft and hydrolysis lignin hydroconversion over unsupported NiMoS catalyst. Chem Eng J 2023;453:139829. https://doi.org/10.1016/j.cej.2022.139829.

[38] Horáček J, Homola F, Kubičková I, Kubička D. Lignin to liquids over sulfided catalysts. Catal Today 2012;179:191–8. https://doi.org/10.1016/j.cattod.2011.06.031.

[39] Wang S, Gao W, Xiao L-P, Shi J, Sun R-C, Song G. Hydrogenolysis of biorefinery corncob lignin into aromatic phenols over activated carbon-supported nickel, Sustainable. Energy Fuels 2019;3:401–8. https://doi.org/10.1039/C8SE00359A.

[40] Tymchyshyn M, Rezayan A, Yuan Z, Zhang Y, C.. (Charles) Xu, Reductive hydroprocessing of hydrolysis lignin over efficient bimetallic catalyst MoRu/AC. Ind Eng Chem Res 2020. https://doi.org/10.1021/acs.iecr.0c01151.

[41] Sang Y, Chen M, Yan F, Wu K, Bai Y, Liu Q, et al. Catalytic Depolymerization of Enzymatic Hydrolysis Lignin into Monomers over an Unsupported Nickel Catalyst in Supercritical Ethanol. Ind Eng Chem Res 2020;59:7466–74. https://doi.org/10.1021/acs.iecr.0c00812.

[42] Soave G. Equilibrium constants from a modified Redlich-Kwong equation of state. Chem Eng Sci 1972;27:1197–203. https://doi.org/10.1016/0009-2509(72)80096-4.

[43] Perry S, Perry RH, Green DW, Maloney JO. Perry's chemical engineers' handbook 2000. https://doi.org/10.5860/choice.38-0966.

[44] Wang R, Smith KJ. Preparation of Unsupported NiMoP Catalysts for 4,6-Dimethyldibenzothiophene Hydrodesulfurization. Catal Letters 2014;144:1594–601. https://doi.org/10.1007/s10562-014-1290-9.

[45] Thommes M, Kaneko K, Neimark AV, Olivier JP, Rodriguez-Reinoso F, Rouquerol J, et al. Physisorption of gases, with special reference to the evaluation of surface area and pore size distribution (IUPAC Technical Report). Pure Appl Chem 2015;87:1051–69. https://doi.org/10.1515/pac-2014-1117.

[46] Li Y, Fu J, Chen B. Highly selective hydrodeoxygenation of anisole, phenol and guaiacol to benzene over nickel phosphide. RSC Adv 2017;7:15272–7. https://doi.org/10.1039/C7RA00989E.

[47] Moon J-S, Kim E-G, Lee Y-K. Active sites of Ni2P/SiO2 catalyst for hydrodeoxygenation of guaiacol: A joint XAFS and DFT study. J Catal 2014;311:144–52. https://doi.org/10.1016/j.jcat.2013.11.023.

[48] Alvarez-Galvan MC, Campos-Martin JM, Fierro JLG. Transition Metal Phosphides for the Catalytic Hydrodeoxygenation of Waste Oils into Green Diesel. Catalysts 2019;9. https://doi.org/10.3390/catal9030293.

[49] Petrov D, Angelov B, Lovchinov V. Magnetic and XPS studies of lithium lanthanide tetraphosphates LiLnP4O12 (Ln=Nd, Gd, Er). J Rare Earths 2013;31:485–9. https://doi.org/10.1016/S1002-0721(12)60307-X.

[50] Zhou D, Cheng P, Luo J, Xu W, Li J, Yuan D. Facile synthesis of graphene@NiMoO4 nanosheet arrays on Ni foam for a high-performance asymmetric supercapacitor. J Mater Sci 2017;52:13909–19. https://doi.org/10.1007/s10853-017-1467-x.

[51] Ročnik T, Likozar B, Jasiukaitytė-Grojzdek E, Grilc M. Catalytic lignin valorisation by depolymerisation, hydrogenation, demethylation and hydrodeoxygenation: Mechanism, chemical reaction kinetics and transport phenomena. Chem Eng J 2022;448:137309. https://doi.org/10.1016/j.cej.2022.137309.

[52] Kimura K, Saika Y, Kakuta Y, Kurihara K. Catalytic transfer hydrogenation of cellulose to hydrocarbons using straight-chain aliphatic hydrocarbon as a solvent. Biomass Convers Biorefin 2021;11:873–84. https://doi.org/10.1007/s13399-020-01206-x.

[53] Gueudré L, Chapon F, Mirodatos C, Schuurman Y, Venderbosch R, Jordan E, et al. Optimizing the bio-gasoline quantity and quality in fluid catalytic cracking co-refining. Fuel 2017;192:60–70. https://doi.org/10.1016/j.fuel.2016.12.021.

[54] van Niekerk AS, Drew B, Larsen N, Kay PJ. Influence of blends of diesel and renewable fuels on compression ignition engine emissions over transient engine conditions. Appl Energy 2019;255:113890. https://doi.org/10.1016/j.apenergy.2019.113890.

[55] Gutiérrez-Rubio S, Berenguer A, Přech J, Opanasenko M, Ochoa-Hernández C, Pizarro P, et al. Guaiacol hydrodeoxygenation over Ni2P supported on 2D-zeolites. Catal Today 2020;345:48–58. https://doi.org/10.1016/j.cattod.2019.11.015.

[56] Han X, Wang H, Zeng Y, Liu J. Advancing the application of bio-oils by co-processing with petroleum intermediates: A review. Energy Convers Manage: X 2021;10:100069. https://doi.org/10.1016/j.ecmx.2020.100069.

[57] Sousa-Aguiar EF, Ximenes VL, de Almeida JM, Romano PN, Carvalho Y. Catalysts for Co-processing Biomass in Oil Refining Industry. In: Sustainable Catalysis for Biorefineries. The Royal Society of Chemistry; 2018. https://doi.org/10.1039/9781788013567-00001.

[58] Bergvall N, Sandström L, Cheah YW, Öhrman OGW. Slurry Hydroconversion of Solid Kraft Lignin to Liquid Products Using Molybdenum- and Iron-Based Catalysts. Energy Fuel 2022;36:10226–42. https://doi.org/10.1021/acs.energyfuels.2c01664.

[59] Dyson PJ, Jessop PG. Solvent effects in catalysis: rational improvements of catalysts via manipulation of solvent interactions, Catal. Sci Technol 2016;6:3302–16. https://doi.org/10.1039/C5CY02197A.

[60] Haruna AM, Meredith W, Snape CE. Synergistic effect in co-processing a residue from a transesterification process with vacuum gas oil in fluid catalytic cracking. Fuel 2022;327:124973. https://doi.org/10.1016/j.fuel.2022.124973.

[61] Barbier J, Charon N, Dupassieux N, Loppinet-Serani A, Mahé L, Ponthus J, et al. Hydrothermal conversion of lignin compounds. A detailed study of fragmentation and condensation reaction pathways, Biomass Bioenergy 2012;46:479–91. https://doi.org/10.1016/j.biombioe.2012.07.011.

[62] Oregui-Bengoechea M, Gandarias I, Arias PL, Barth T. Solvent and catalyst effect in the formic acid aided lignin-to-liquids. Bioresour Technol 2018;270:529–36. https://doi.org/10.1016/j.biortech.2018.09.062.

[63] Osorio Velasco J, Van Der Linden I, Deuss PJ, Heeres HJ. Efficient depolymerization of lignins to alkylphenols using phosphided NiMo catalysts, Catal. Sci Technol 2021;11:5158–70. https://doi.org/10.1039/D1CY00588J.

[64] Joffres B, Lorentz C, Vidalie M, Laurenti D, Quoineaud AA, Charon N, et al. Catalytic hydroconversion of a wheat straw soda lignin: Characterization of the products and the lignin residue. Appl Catal B 2014;145:167–76. https://doi.org/10.1016/j.apcatb.2013.01.039.

[65] Azadi P, Inderwildi OR, Farnood R, King DA. Liquid fuels, hydrogen and chemicals from lignin: A critical review. Renew Sustain Energy Rev 2013;21:506–23. https://doi.org/10.1016/j.rser.2012.12.022.

[66] Van den Bosch S, Koelewijn SF, Renders T, Van den Bossche G, Vangeel T, Schutyser W, et al. Catalytic Strategies Towards Lignin-Derived Chemicals. Springer International Publishing 2018. https://doi.org/10.1007/s41061-018-0214-3.

[67] D. Munick de Albuquerque Fragoso, F.P. Bouxin, J.R.D. Montgomery, N.J. Westwood, S.D. Jackson, Catalytic depolymerisation of isolated lignin to fine chemicals: Depolymerisation of Kraft lignin, Bioresour Technol Rep 9 (2020) 100400. doi: 10.1016/j.biteb.2020.100400.

[68] Badoga S, Alvarez-Majmutov A, Xing T, Gieleciak R, Chen J. Co-processing of Hydrothermal Liquefaction Biocrude with Vacuum Gas Oil through Hydrotreating and Hydrocracking to Produce Low-Carbon Fuels. Energy Fuel 2020;34:7160–9. https://doi.org/10.1021/acs.energyfuels.0c00937.

[69] Al-Sabawi M, Chen J. Hydroprocessing of biomass-derived oils and their blends with petroleum feedstocks: A review. Energy Fuel 2012;26:5373–99. https://doi.org/10.1021/ef3006405.

[70] den Bosch S, Schutyser W, Vanholme R, Driessen T, Koelewijn S-F, Renders T, et al. Reductive lignocellulose fractionation into soluble lignin-derived phenolic monomers and dimers and processable carbohydrate pulps. Energy Environ Sci 2015;8:1748–63. https://doi.org/10.1039/C5EE00204D.